Reflection of Nonlinear Baroclinic Rossby Waves and the Driving of Secondary Mean Flows

FEDERICO GRAEF

Centro de Investigación Científica y de Educación Superior de Ensenada, Ensenada, Baja California, Mexico

LORENZ MAGAARD

Department of Oceanography, University of Hawaii, Honolulu, Hawaii

(Manuscript received 12 March 1993, in final form 16 November 1993)

ABSTRACT

The reflection of weakly nonlinear Rossby waves (RWs) from a vertical wall is examined analytically through perturbation methods, with the β-Rossby number (ϵ) as the small parameter. A uniformly valid solution up to $O(\epsilon^3)$ is constructed using multiple scales. At $O(\epsilon)$, the nonlinear interaction between an incident and the reflected RW leads to 1) an Eulerian steady flow, $u_s^{(1)}$, parallel to the (nonzonal) wall and 2) a transient flow oscillating with a frequency twice (2ω) that of the RW pair. The steady forcing, whose response is $u_s^{(1)}$, can never be resonant, which implies, under the weak nonlinear regime, that $u_s^{(1)}$ is stable to the driving RWs. At the next order, the nonlinear interaction between the incident–reflected RW pair and $u_s^{(1)}$ plus the transient flow produces, in general, resonant forcing leading to a modification of the RWs' phases: a shift in their offshore wavenumber. The steady flow that occurs at $O(\epsilon^3)$ is driven by the modified RWs as well as through interactions of several components of the solution up to second order; it is the next correction to $u_s^{(1)}$. This correction can be significant for reasonable wave parameters that allow, at the same time, a meaningful perturbative solution. The entire steady circulation induced by the nonlinear dynamics, up to $O(\epsilon^3)$, is immune to resonances for $|\sin\alpha| > 1/3$, where α is the angle between the wall and the circles of latitude [except for the resonance that occurs at $O(\epsilon^2)$]. Thus, the waves produce a mean current, the mean current affects the waves, which change the current, and so on. There is new observational evidence of the existence of the North Hawaiian Ridge Current (Mysak and Magaard), which has been hypothesized as an RW-driven current.

1. Introduction

Mysak and Magaard (1983; hereafter MM) showed that the reflection of baroclinic Rossby waves (RWs) from a nonzonal wall leads to the generation of a steady Eulerian mean flow (secondary flow) parallel to the wall. The authors incorporated Rayleigh friction in their analytical model to reduce the inviscid flow to realistic values; however, it is not a necessary ingredient for the production of the steady flow. The theoretically predicted secondary flow was computed using the field of baroclinic RWs incident on the Hawaiian Ridge (Magaard 1983) and compared fairly well with the surface flow field found in White's (1983) analysis of historical hydrographic and XBT data. Oh and Magaard (1984) added lateral friction to MM's model, producing smaller Eulerian mean current speeds but wider current bands. Sun ėt al. (1988) applied Oh and Magaard's model to the Hawaiian Ridge with both Rayleigh and lateral friction coefficients determined by a least-squares fit to the high-resolution hydrographic observations of Roden (1985). The authors concluded that the model fits the data reasonably well.

The data used for the comparisons between theory and observations in MM, Oh and Magaard (1984), and Sun et al. (1988) did not allow an averaging along the ridge or a time averaging, but the authors justified that such comparisons were meaningful because the steady current was an order of magnitude larger than the currents associated with the Rossby waves. We will show in this paper that this statement is not correct due to the transients, and that a fair comparison between the theoretically predicted mean current and observations requires data that allow an average along the ridge or over time. Preliminary results from a dataset of these characteristics have been made available to us by Firing (1993, personal communication). Measurements of the currents on the northeastern side of the Hawaiian Ridge averaged over a period from October 1988 through January 1993 show significant resemblance to the current (North Hawaiian Ridge Current) predicted by MM. We consider these measurements to be the first evidence that this current actually exists.

Corresponding author address: Dr. Federico Graef, CICESE, P.O. Box 434844, San Diego, CA 92143-4844.

The main shortcoming of MM theory is that it neglects the influence of the secondary steady mean flow on the driving RW fields, both incoming and reflected. The theory developed here studies this influence and addresses two additional questions: the stability of the RW-driven steady flow and the poor comparisons in some instances between theory and observations. It investigates also whether the reflection problem of RWs can be strongly nonlinear when more or less realistic wave parameters [obtained from the observed RWs, for example, from Kang and Magaard (1980)] produce a β-Rossby number of the reflected RW (for western boundaries) that is of the order or larger than one.

Higher-order nonlinearities produce new contributions to the steady flow of MM, which should provide a more accurate steady circulation resulting from the nonlinear interactions in the reflection problem.

The ocean model is kept very simple in order to focus attention on the complications introduced by higher-order nonlinearities. The model is quasigeostrophic (QG) on a semi-infinite oceanic β plane bounded by an infinite lateral straight boundary, has a flat bottom, no friction, and no external forcing.

This paper is organized as follows. Section 2 presents the formulation of the reflection problem and the solution up to first order in the β-Rossby number expansion. By definition, the "effect" of the RW-driven steady flow on the waves themselves occurs at second order in our perturbation scheme, which is examined in section 3. Section 4 poses the third-order problem but only the steady response is calculated, which is precisely the next higher-order correction to MM's steady flow. Observational evidence and numerical applications [e.g., the first-order steady flow (MM's flow in the absence of friction) is compared to the steady flow up to third order] with some oceanographic implications are presented in section 5. The last section is devoted to discussion and conclusions. The appendix includes details of the third-order problem.

2. Formulation of the problem and solution up to first order

a. Governing equation and boundary conditions

The governing equation is the QG potential vorticity equation (QGPVE), which in *nondimensional* form and using a coordinate system with x parallel, y perpendicular to the wall, and z vertically upward, takes the form

$$[\partial_t + \epsilon J(\psi,\cdot)]\left\{\nabla^2\psi + \partial_z\left[\frac{1}{S(z)}\,\partial_z\psi\right]\right\} + \cos\alpha\partial_x\psi + \sin\alpha\partial_y\psi = 0. \quad (2.1)$$

Here, $\nabla^2 = \partial_x\partial_x + \partial_y\partial_y$, $J(A, B) \equiv (\partial_x A)(\partial_y B) - (\partial_y A)(\partial_x B)$ is the Jacobian operator, t is the nondimensional time, ψ the QG streamfunction, α the angle that the wall makes with the circles of latitude, $\epsilon = U/(\beta L^2)$ the β-Rossby number, and $S(z) = H^2N^2(z)/f_0^2L^2$ the stratification parameter (Pedlosky 1979), where L and U are horizontal length and velocity scales, β is the northward gradient of the planetary vorticity, f_0 is the Coriolis parameter, H is the water depth, and $N(z)$ is the Brunt–Väisälä frequency.

The scales L and U have been used to introduce the nondimensional variables of (2.1) as follows: $(x, y, z, t, \psi) = [x_*/L, y_*/L, z_*/H, \beta L t_*, \psi_*/(UL)]$, where the time has been scaled by the Rossby wave period. Dimensional variables are denoted with an asterisk as subscript.

Since (2.1) holds in the domain $-\infty < x < \infty$, $y > 0$, $-1 < z < 0$, the following boundary conditions (BCs) must also be imposed.

- No normal flow at the reflecting wall; that is, $\partial_x\psi = 0$ at $y = 0$.
- No normal flow at a flat bottom and at a rigid lid: $[\partial_t + \epsilon J(\psi,\cdot)]\partial_z\psi = 0$ at $z = -1, 0$.
- At infinity ψ must remain bounded and satisfy the radiation condition: the only energy (associated with a homogeneous QGPVE) approaching the boundary is that of the incident wave. In other words, when the need arises to supplement a forced solution with a homogeneous solution of the QGPVE (an RW in our case) to satisfy the BC at the wall, the RW chosen must have an energy flux away from the wall, that is, must be a reflected wave. The proposed condition is similarly used in Anderson and Gill (1975).

In the weakly nonlinear theory of midlatitude RWs, a perturbative solution for the QG streamfunction is sought in the form $\psi = \psi^{(0)} + \epsilon\psi^{(1)} + \epsilon^2\psi^{(2)} + \cdots$.

b. Zeroth order

A solution to the zeroth-order problem is given as a superposition of an incident and a reflected RW (LeBlond and Mysak 1978; Pedlosky 1979):

$$\psi^{(0)} = A\Psi_n(z)(\cos\theta_1^{(0)} - \cos\theta_2^{(0)}), \quad (2.2)$$

where $\theta_i^{(0)} \equiv kx + l_i y - \omega t + \phi$, $i = 1, 2$,

$$\omega = \sigma_n(k, l_i) \equiv \frac{-(k\cos\alpha + l_i\sin\alpha)}{k^2 + l_i^2 + L^2 f_0^2 \lambda_n}, \quad i = 1, 2, \quad (2.3)$$

A is the wave amplitude, ϕ is an arbitrary constant phase, and $\Psi_n(z)$ is an eigenfunction of the vertical Sturm–Liouville problem with corresponding eigenvalue λ_n. The offshore wavenumbers $l_{1,2}$ are the real roots of (2.3) when vertical mode number n, frequency ω, and wavenumber component along the wall k are given. The root with the positive (negative) radical, chosen to be l_1 (l_2), corresponds to the incident (reflected) wave for all boundary orientations (Graef-Ziehl 1990; hereinafter GZ). If the roots $l_{1,2}$ are equal or complex, the solution is unbounded with a linear growth in y in the first case and an exponential growth away from the wall in the second case (GZ).

c. First order

The first-order $[O(\epsilon)]$ perturbation equations are

$$\partial_t\left\{\nabla^2\psi^{(1)} + \partial_z\left[\frac{1}{S(z)}\partial_z\psi^{(1)}\right]\right\} + \cos\alpha\partial_x\psi^{(1)} + \sin\alpha\partial_y\psi^{(1)} = -B_{12}\Psi_n^2(z)[\cos(\theta_1^{(0)} - \theta_2^{(0)}) - \cos(\theta_1^{(0)} + \theta_2^{(0)})], \quad (2.4)$$

where $B_{12} \equiv \frac{1}{2}A^2k(l_1 - l_2)(l_1^2 - l_2^2)$,

$$\partial_x\psi^{(1)} = 0 \quad \text{at} \quad y = 0, \quad (2.5)$$

$$\partial_t\partial_z\psi^{(1)} = 0 \quad \text{at} \quad z = -1, 0, \quad (2.6)$$

$$\psi^{(1)} \quad \text{bounded as} \quad x \to \pm\infty, y \to \infty, \quad (2.7)$$

and the radiation condition remains in effect. Note that $J(\psi^{(0)}, \partial_z\psi^{(0)}) \equiv 0$.

Henceforth we will assume that $B_{12} \neq 0$. For $A \neq 0$ this is equivalent to assume that $k \neq 0$ and $|l_1| \neq |l_2|$ (i.e., $\sin\alpha \neq 0$).

Since the problem for $\psi^{(1)}$ is a linear, forced problem, the solution can be written as $\psi^{(1)} = \psi_{p1}^{(1)} + \psi_{p2}^{(1)} + \psi_{\text{hom}}^{(1)}$, where

$$\psi_{p1}^{(1)} = -\frac{B_{12}\Psi_n^2(z)}{(l_1 - l_2)\sin\alpha}\sin[(l_1 - l_2)y] \quad (2.8)$$

is the steady forced solution that gives the MM flow for their special case of no friction,

$$\psi_{p2}^{(1)} = \sum_{m=0}^{\infty}\frac{b_m}{\lambda - L^2f_0^2\lambda_m}\Psi_m(z)\sin(\theta_1^{(0)} + \theta_2^{(0)}) \equiv F(z)\sin(\theta_1^{(0)} + \theta_2^{(0)}), \quad (2.9)$$

in which $b_m = -B_{12}\int_{-1}^{0}\Psi_n^2\Psi_m dz/(2\omega) \equiv -B_{12}\xi_{nnm}/(2\omega)$ and

$$\lambda \equiv -\left\{(2k)^2 + (l_1 + l_2)^2 + \frac{1}{2\omega}[2k\cos\alpha + (l_1 + l_2)\sin\alpha]\right\}, \quad (2.10)$$

and $\psi_{\text{hom}}^{(1)}$ is a homogeneous solution of (2.4), which is chosen to satisfy (2.5). It is given by

$$\psi_{\text{hom}}^{(1)} = -\sum_{m=0}^{m_c-1}\frac{b_m}{\lambda - L^2f_0^2\lambda_m}\Psi_m(z) \times \sin(2kx + \eta_{m2}y - 2\omega t + 2\phi) - \sum_{m=m_c}^{\infty}\frac{b_m}{\lambda - L^2f_0^2\lambda_m}\Psi_m(z)e^{-\eta_m^{(i)}y} \times \sin(2kx + \eta_m^{(r)}y - 2\omega t + 2\phi), \quad (2.11)$$

where $2\omega = \sigma_m(2k, \eta_m)$, $m = 0, 1, 2, \ldots,$

$$\eta_{m2} = -\frac{\sin\alpha}{4\omega} - \left[\frac{1}{16\omega^2} - L^2f_0^2\lambda_m - \left(2k + \frac{\cos\alpha}{4\omega}\right)^2\right]^{1/2}, \quad (2.12)$$

m_c is the smallest m such that the radicand in (2.12) becomes negative, $\eta_m^{(r)} = -\sin\alpha/(4\omega)$, and $\eta_m^{(i)} = \{L^2f_0^2\lambda_m + [2k + \cos\alpha/(4\omega)]^2 - 1/(16\omega^2)\}^{1/2}$.

d. Discussion of first-order solution

1) STEADY PART

Since $u^{(1)} = -\partial_y\psi^{(1)}$, the steady Eulerian mean flow is

$$u_s^{(1)}(y, z) = -\partial_y\psi_{p1}^{(1)} = \frac{B_{12}}{\sin\alpha}\Psi_n^2(z)\cos[(l_1 - l_2)y], \quad (2.13)$$

or in dimensional form, which simply means multiplying (2.13) by $\epsilon U = U^2/(\beta L^2)$, it is

$$u_{s*}^{(1)}(y_*, z_*) = \frac{B_{12*}}{\beta\sin\alpha}\Psi_n^2(z_*)\cos[(l_{1*} - l_{2*})y_*], \quad (2.14)$$

where $B_{12*} \equiv A_*^2k_*(l_{1*} - l_{2*})(l_{1*}^2 - l_{2*}^2)/2$ and $A_* = ULA$.

It is noteworthy that in the inviscid case, the Eulerian steady flow $u_s^{(1)}$ has exactly the same magnitude as the Stokes drift produced by the incident–reflected RWs but of opposite sign, yielding a *zero* Lagrangian mean flow (MM).

The production of a steady flow parallel to the boundary occurs only for nonzonal walls; this result holds true for any number of arbitrary incident–reflected RW pairs. However, the steadiness of the current alone, generated by the nonlinear interaction of incident–reflected RWs, can happen in zonal walls. Consider a zonal wall and imagine we choose, for example, *two* incident–reflected RW pairs with the same n and ω, that is, on the same (n, ω) circle. We would obtain two nonzero steady forcing terms (four terms combined into two) with a nonzero zonal wavenumber. These steady forcing terms would drive, in general, a nonzonal steady flow; that is, a steady flow not parallel to the wall, but whose normal component vanishes at the (zonal) wall. This is perhaps not a coincidence, since otherwise (2.5) cannot be satisfied, because the only homogeneous and steady solution of the linear QGPVE is a zonal flow.

A time-independent forcing term with zero zonal wavenumber requires two interacting RWs of the same frequency and of the same zonal wavenumber; but this is impossible, for such two waves will not interact! This proves that the steady forcing is *never resonant,* which has the following important consequence: *the steady flow is stable* when the nonlinear effects are weak, since in such a case, instability proceeds only via resonant interactions (Gill 1974; Plumb 1977). There cannot be energy exchange between $u_s^{(1)}$ and the "parent" RW pair(s); the steady flow is neutrally stable to these RWs. But we cannot say whether the steady flow is stable to "other" disturbances, and whether it makes sense to disregard the RWs, sources of the flow. Pedlosky (1979; pp. 425) comments on this point:

> . . . Consequently the structure of the observed mean flow already implicitly assumes the existence of fluctuations, and it is a generally misleading fiction to suppose that the stability of the averaged state accurately portrays the stability of the fluctuation-free states, since *in most cases the nature of the fluctuations alters the fluctuation-free state in the direction of stability*. . .

Technically, of course, one could study the stability of the RW-driven steady flow. We have a brief discussion on this in the last section.

In MM, friction acted only upon the short reflected wave (for western boundaries). Mathematically it meant to have l_2 complex, so the reflected wave had an exponentially decaying amplitude away from the wall. With such friction, the forcing for $\psi^{(1)}$ in our problem would have an exponentially decaying (in y) factor. Consequently, the steady flow would be exponentially decaying away from the wall and thus would be a boundary current, as found by MM.

2) TRANSIENT PART

Clearly, solution (2.9) is valid when λ is not one of the eigenvalues $L^2 f_0^2 \lambda_m$. If λ is an eigenvalue, say $\lambda = L^2 f_0^2 \lambda_M$, $\Psi_M(z)$ is the corresponding eigenfunction and if $\xi_{nnM} = 0$—that is, if there is no projection of the vertical structure of the forcing onto the Mth mode—then there is a solution of the form (2.9) with

$$F(z) = c\Psi_M(z) + \sum_{\substack{m=0 \\ m\neq M}}^{\infty} \frac{b_m}{L^2 f_0^2(\lambda_M - \lambda_m)} \Psi_m(z), \tag{2.15}$$

where c is an *arbitrary* constant, thus giving an infinite number of solutions. The case $\lambda = L^2 f_0^2 \lambda_M$ and $\xi_{nnM} \neq 0$ is resonant, although to have a solution of the resonance conditions with k real it is necessary that $|\sin\alpha| \leq 1/3$ (Graef 1993).

In (2.11), each RW mode has parameters m, 2ω, and $2k$; the dispersion relation then yields two offshore wavenumbers, $\eta_{m1,2}$, of which only one is chosen either as the reflected RW (using the radiation condition) if $\eta_{m1,2}$ are real, or as the exponentially decaying RW (use the boundedness of $\psi^{(1)}$) if $\eta_{m1,2}$ are complex.

We note that m_c could be zero or that $\eta_{m1,2}$ could be complex $\forall m$, since one cannot show in general by using the inequality $|k + \cos\alpha/(2\omega)| < [1/(4\omega^2) - L^2 f_0^2 \lambda_n]^{1/2}$, or equivalently $l_{1,2}$ real and different, whether $\eta_{01,2}$ are real or complex.

If the incident and reflected wave are relatively short (for given n and ω), then the response is an exponentially decaying oscillation in y, trapped to the wall. The higher the baroclinic mode, the shorter the length scale of decay is and the smaller its amplitude, which should decrease faster than $1/m^2$. We have that $\eta_m^{(i)} y \sim L f_0 \lambda_m^{1/2} y = y_*/r_{i,m}$ for large m, where $r_{i,m} = 1/(f_0 \lambda_m^{1/2})$ is the mth mode internal Rossby radius of deformation. Thus, for large m, the length scale of decay (of that mode) is given approximately by $r_{i,m}$. On the other hand, if the wavelengths of the incident–reflected RW pair are relatively long, then *part* of the response is oscillatory in y and the rest is trapped.

In summary, the response to the transient or 2ω forcing consists of two parts.

1) Physically, the 2ω forcing induces a flow ($\psi_{p2}^{(1)}$) that does not satisfy the physical constraints on the motion. This is a direct response, whose phase lies at 90° from that of the forcing.

2) The fluid then adjusts by generating free RWs to balance out the forced flow normal to the wall ($\psi_{\text{hom}}^{(1)}$); these waves must have outgoing energy flux, that is, must be reflected, or exponentially decaying away from the boundary. This is the indirect response.

Our first-order solution is then (for λ not an eigenvalue) given by the sum of (2.8), (2.9), and (2.11); that is,

$$\begin{aligned}\psi^{(1)} = &-\sum_{m=0}^{m_c-1} \frac{b_m \Psi_m(z)}{\lambda - L^2 f_0^2 \lambda_m} \sin\theta_{m2}^{(1)} \\ &- \sum_{m=m_c}^{\infty} \frac{b_m \Psi_m(z)}{\lambda - L^2 f_0^2 \lambda_m} e^{-\eta_m^{(i)} y} \sin\theta_{mr}^{(1)} \\ &- \frac{B_{12}\Psi_n^2(z)}{(l_1 - l_2)\sin\alpha} \sin[(l_1 - l_2)y] \\ &+ \sum_{m=0}^{\infty} \frac{b_m \Psi_m(z)}{\lambda - L^2 f_0^2 \lambda_m} \sin(\theta_1^{(0)} + \theta_2^{(0)}),\end{aligned} \tag{2.16}$$

where we have introduced the abbreviations

$$\theta_{m2}^{(1)} \equiv 2kx + \eta_{m2} y - 2\omega t + 2\phi, \tag{2.17}$$

$$\theta_{mr}^{(1)} \equiv 2kx + \eta_m^{(r)} y - 2\omega t + 2\phi. \tag{2.18}$$

As indicated in (2.4), the series in (2.16) and their partial derivatives up to second order must be uniformly convergent in order to differentiate $\psi^{(1)}$ term by term (this has been checked).

e. Barotropic case

The first-order solution just presented is quite general inasmuch as it is valid for any arbitrary oceanic stratification.

To obtain the first-order solution in the particular case that the incident–reflected pair is barotropic, we put $n = 0$ into the equations. Then $b_m = -B_{12}\delta_{m0}/(2\omega)$ and the infinite series in (2.16) become each a single term. The solution is then

$$\psi^{(1)} = \psi^{(1)}_{\text{hom}} - \frac{B_{12}}{(l_1 - l_2)\sin\alpha}\sin[(l_1 - l_2)y] + \frac{b_0}{\lambda - L^2 f_0^2 \lambda_0}\sin(\theta_1^{(0)} + \theta_2^{(0)}), \quad (2.19)$$

where

$$\psi^{(1)}_{\text{hom}} = -\frac{b_0}{\lambda - L^2 f_0^2 \lambda_0}\begin{cases} \sin\theta_{02}^{(1)}, & k_- \leqslant k \leqslant k_+ \\ e^{-\eta_0^{(i)} y}\sin\theta_{0r}^{(1)}, & k < k_- \\ & \text{or } k > k_+, \end{cases} \quad (2.20)$$

in which $k_\pm = \frac{1}{2}\{-\cos\alpha/(4\omega) \pm [1/(16\omega^2) - L^2 f_0^2 \lambda_0]^{1/2}\}$. For a rigid lid, $\lambda_0 = 0$ and for a free surface, $\lambda_0 = 1/(gH)$.

All baroclinic modes disappear from the first-order solution when the incident–reflected RW pair is barotropic, since the interaction of two barotropic waves cannot excite baroclinic modes.

3. Second-order problem and solution

A major limitation of MM theory is the absence of any influence of the RW-driven steady flow on the RWs themselves. By definition, such influence must appear at second order. If we succeed in solving the second-order perturbation equations, we must be able to determine what happens to the incoming–reflected waves when they encounter the steady flow, whether there are second-order resonances, and if so, whether they are inhibited by the orientation of the wall.

The second order problem is

$$\partial_t\left\{\nabla^2\psi^{(2)} + \partial_z\left[\frac{1}{S(z)}\partial_z\psi^{(2)}\right]\right\} + \cos\alpha\partial_x\psi^{(2)} + \sin\alpha\partial_y\psi^{(2)} = -\mathcal{F}$$

$$\equiv -J\left\{\psi^{(0)}, \nabla^2\psi^{(1)} + \partial_z\left[\frac{1}{S(z)}\partial_z\psi^{(1)}\right]\right\} - J\left\{\psi^{(1)}, \nabla^2\psi^{(0)} + \partial_z\left[\frac{1}{S(z)}\partial_z\psi^{(0)}\right]\right\} \quad (3.1)$$

$$\partial_x\psi^{(2)} = 0 \quad \text{at} \quad y = 0 \quad (3.2)$$

$$\partial_t\partial_z\psi^{(2)} = -J(\psi^{(0)}, \partial_z\psi^{(1)}) - J(\psi^{(1)}, \partial_z\psi^{(0)}) = 0 \quad \text{at} \quad z = -1, 0 \quad (3.3)$$

$$\psi^{(2)} \quad \text{bounded as} \quad x \to \pm\infty, y \to \infty. \quad (3.4)$$

The forcing for $\psi^{(2)}$, being the rhs of (3.1), in which the RWs advect the vorticity of the steady flow plus transients, and vice versa, is

$$\begin{aligned}\mathcal{F} = A\Psi_n k\Bigg\{&\frac{B_{12}\cos[(l_1 - l_2)y]}{\sin\alpha}\sum_{i=1}^{2}(-1)^i\left[(\delta_{i1}l_2^2 + \delta_{i2}l_1^2 - 2l_1 l_2 - k^2 - L^2 f_0^2\lambda_n)\Psi_n^2 - \frac{d}{dz}\left(\frac{1}{S}\frac{d\Psi_n^2}{dz}\right)\right] \\ &\times \sin\theta_i^{(0)} - \sum_{m=0}^{m_c - 1}\gamma_m\Psi_m\sum_{i=1}^{2}(-1)^i\frac{\sin\alpha}{2\omega}(\eta_{m2} - 2l_i)^2\sin\theta_i^{(0)}\cos\theta_{m2}^{(1)} \\ &- \sum_{m=m_c}^{\infty}\gamma_m\Psi_m e^{-\eta_m^{(i)}y}\sum_{i=1}^{2}(-1)^i\frac{\sin\alpha}{\omega}\sin\theta_i^{(0)}\left\{\eta_m^{(i)}(2l_i - \eta_m^{(r)})\sin\theta_{mr}^{(1)} + \frac{1}{2}[(\eta_m^{(r)} - 2l_i)^2 - \eta_m^{(i)2}]\cos\theta_{mr}^{(1)}\right\} \\ &- (l_1 - l_2)\cos(\theta_1^{(0)} + \theta_2^{(0)})\sum_{m=0}^{\infty}\gamma_m\Psi_m\sum_{i=1}^{2}\sin\theta_i^{(0)}\left[(-1)^{i-1}\frac{\sin\alpha}{2\omega}(l_1 - l_2) + L^2 f_0^2\lambda_m - \lambda\right]\Bigg\} \\ = \frac{1}{2}&Ak\Psi_n\{F_1(z)\sin\theta_1^{(0)} + F_2(z)\sin\theta_2^{(0)} + F_3(z)\sin(2\theta_1^{(0)} - \theta_2^{(0)}) + F_4(z)\sin(2\theta_2^{(0)} - \theta_1^{(0)}) \\ &+ F_5(z)\sin(2\theta_1^{(0)} + \theta_2^{(0)}) + F_6(z)\sin(2\theta_2^{(0)} + \theta_1^{(0)}) + \cdots\}, \quad (3.5)\end{aligned}$$

where the first two coefficients in the last equality are

$$\begin{aligned}F_i(z) = \frac{B_{12}(-1)^{i-1}}{\sin\alpha}&\left[(l_i^2 - 2l_1 l_2 - k^2 - L^2 f_0^2\lambda_n)\Psi_n^2 - \frac{d}{dz}\left(\frac{1}{S}\frac{d\Psi_n^2}{dz}\right)\right] \\ &+ (l_1 - l_2)\sum_{m=0}^{\infty}\gamma_m\Psi_m\left[(-1)^i\frac{\sin\alpha}{2\omega}(l_1 - l_2) + L^2 f_0^2\lambda_m - \lambda\right], \quad i = 1, 2. \quad (3.6)\end{aligned}$$

To arrive at (3.5), we used the dispersion relations (2.3) and $2\omega = \sigma_m(2k, \eta_m)$ repeatedly, as well as the definitions of λ and $\eta_m^{(r)}$, and introduced the abbreviation $\gamma_m \equiv b_m/(\lambda - L^2 f_0^2 \lambda_m) = -B_{12}\xi_{nnm}/[2\omega(\lambda - L^2 f_0^2\lambda_m)]$.

a. Secular terms

Although the x, y, t dependence of the forcing terms proportional to $\sin\theta_i^{(0)}$, $i = 1, 2$, is that of the incident RW for $i = 1$ (and reflected for $i = 2$), it is not immediately obvious whether these terms are resonant, since we need to check if their z dependence has some nth mode (recall that the incident–reflected RW pair is nth mode).

Using the Sturm–Liouville (SL) series expansion of Ψ_n^2, $\sum_{m=0}^{\infty} \xi_{nnm}\Psi_m$, it is straightforward to show that $F_1(z) + F_2(z) \equiv 0$. Then the terms whose secularity is being investigated are proportional to $F_1(z)(\sin\theta_1^{(0)} - \sin\theta_2^{(0)})$, so that more and more these two forcing terms resemble the incident–reflected RW pair we started with, except for the amplitude and a phase change of $\pi/2$.

The solution to (3.1) will be sought in terms of a SL series expansion. We write

$$\psi^{(2)} = \sum_{l=0}^{\infty} \Phi_l^{(2)}(x, y, t)\Psi_l(z), \quad (3.7)$$

where $\Phi_l^{(2)} = \int_{-1}^{0} \psi^{(2)}\Psi_l(z)dz$. The equation governing $\Phi_l^{(2)}$ is obtained by multiplying (3.1) by Ψ_l and integrating over the depth. It is written symbolically as

$$\mathcal{M}_l[\Phi_l^{(2)}] = -Ak\int_{-1}^{0} \Psi_l(z)\Psi_n(z)\{\cdots\}dz, \quad (3.8)$$

where the linear operator $\mathcal{M}_l$ is defined by

$$\mathcal{M}_l \equiv \partial_t(\nabla^2 - L^2 f_0^2\lambda_l) + \cos\alpha\partial_x + \sin\alpha\partial_y, \quad (3.9)$$

and the dots within braces indicate that the corresponding lengthy expression on the rhs of (3.5) fits there. The BCs (3.3) have been used to derive the equation for $\Phi_l^{(2)}$.

Defining $\xi_{lnnn} \equiv \int_{-1}^{0} \Psi_l\Psi_n^3 dz$ and using that

$$\int_{-1}^{0} \Psi_l\Psi_n \frac{d}{dz}\left(\frac{1}{S}\frac{d\Psi_n^2}{dz}\right)dz = -L^2 f_0^2\left(\frac{1}{3}\lambda_l + \lambda_n\right)\xi_{lnnn} \; (n > 0), \quad (3.10)$$

obtained by integrating by parts several times, the coefficient of the forcing $\sim \sin\theta_1^{(0)} - \sin\theta_2^{(0)}$ is proportional to $B_{12}C_l \equiv \int_{-1}^{0} \Psi_l\Psi_n F_1(z)dz$; that is,

$$C_l = \frac{1}{\sin\alpha}\left[(l_1^2 - 2l_1l_2 - k^2 - L^2 f_0^2\lambda_n)\xi_{lnnn} + L^2 f_0^2\left(\frac{1}{3}\lambda_l + \lambda_n\right)\xi_{lnnn}\right] + (l_1 - l_2)\sum_{m=0}^{\infty} \frac{\xi_{nnm}\xi_{lnm}}{2\omega(\lambda - L^2 f_0^2\lambda_m)} \times \left[\frac{\sin\alpha}{2\omega}(l_1 - l_2) + \lambda - L^2 f_0^2\lambda_m\right]. \quad (3.11)$$

For $l \neq n$ $(=n)$, $\mathcal{M}_l[\sin\theta_i^{(0)}] \neq 0$ $(=0)$, $i = 1, 2$, and $\sin\theta_i^{(0)}$ is not (is) a homogeneous solution of (3.8). Therefore, the forcing proportional to $C_n(\sin\theta_1^{(0)} - \sin\theta_2^{(0)})$ will be secular unless the coefficient C_n vanishes. Here, C_n is given by

$$C_n = \left[\frac{1}{\sin\alpha}\left(l_1^2 - 2l_1l_2 - k^2 + \frac{1}{3}L^2 f_0^2\lambda_n\right) + \frac{(l_1 - l_2)}{2\omega}\right]\xi_{nnnn} + \frac{(l_1 - l_2)^2}{4\omega^2} \times \sin\alpha \sum_{m=0}^{\infty} \frac{\xi_{nnm}^2}{(\lambda - L^2 f_0^2\lambda_m)}, \quad (3.12)$$

where we have used the identity $\sum_{m=0}^{\infty} \xi_{nnm}^2 = \xi_{nnnn}$, obtained by considering the SL series expansion of Ψ_n^2, squaring it and then integrating over depth. In general, $C_n \neq 0$; thus there usually will be resonance. [It is shown in GZ that there are roots k_r (for given ω) that satisfy $C_n = 0$.] Note that the resonant forcing originates in the nonlinear interaction between the incoming–reflected RW pair ($\psi^{(0)}$) and the *forced* first-order solution, given by the steady mean flow ($\psi_{p1}^{(1)}$) plus the transient forced solution ($\psi_{p2}^{(1)}$). It does not involve the homogeneous solution $\psi_{\rm hom}^{(1)}$.

There is an important difference between this resonance at second order, where resonant forcing occurs "naturally," and resonance at first order in ϵ, which, as we mentioned, is possible only if $\lambda = L^2 f_0^2\lambda_M$, $\xi_{nnM} \neq 0$, and $0 < |\sin\alpha| \leq 1/3$.

The particular solution to

$$\mathcal{M}_n[\Phi_n^{(2)}] = -\frac{1}{2}AkB_{12}C_n(\sin\theta_1^{(0)} - \sin\theta_2^{(0)}) \quad (3.13)$$

is given by

$$\Phi_n^{(2)} = -\frac{AkB_{12}C_n}{2\omega(l_1 - l_2)}y(\sin\theta_1^{(0)} + \sin\theta_2^{(0)}); \quad (3.14)$$

that is, it grows linearly away from the boundary (GZ). A uniformly valid solution to $O(\epsilon^2)$ will now be found by using the method of multiple space scales.

b. Multiple scales

The method of multiple scales is described for example in Bender and Orszag (1978) and Nayfeh (1981). The pedestrian expansion solution, which would grow linearly in y, suggests that the amplitudes and phases of the incident–reflected RW pair be functions of

$$Y_2 = \epsilon^2 y, \quad (3.15)$$

a longer space scale, because Y_2 is not negligible when y is of order ϵ^{-2} or larger. The formal procedure consists of assuming a perturbation expansion of the form

$$\psi = \psi^{(0)}(x, y, z, t; Y_2, Y_3, \cdots) + \epsilon\psi^{(1)}(x, y, z, t; Y_2, Y_3, \cdots) + \cdots, \quad (3.16)$$

where $Y_m = \epsilon^m y$, $m = 2, 3, \cdots$. Even though the exact solution ψ is a function of y alone, multiple scale analysis seeks solutions that are functions of the variables y, Y_2, . . . treated as independent variables. It is emphasized that expressing ψ as a function of several y-space variables is an artifice to remove secular terms[1]; the actual solution has y and Y_m related by $Y_m = \epsilon^m y$, so that y and Y_m are ultimately not independent. We do *not* consider the dependence on Y_1 here, since it has been assumed that the first-order solution is nonresonant.

The y derivatives in the QGPVE are transformed according to $\partial_y \rightarrow \partial_y + \epsilon^2\partial_{Y_2} + \cdots$ and $\partial_{yy} \rightarrow \partial_{yy} + 2\epsilon^2\partial_{yY_2} + \cdots$. The first two orders in ϵ of the QGPVE remain unchanged; the $O(\epsilon^2)$ equation has, in addition to the two Jacobians on the rhs of (3.1), the terms $-2\partial_t\partial_{yY_2}\psi^{(0)} - \sin\alpha\partial_{Y_2}\psi^{(0)}$.

The leading-order solution is written now as

$$\psi^{(0)} = A_1(Y_2, \cdots)\Psi_n(z)\cos\theta_1^{(0)} - A_2(Y_2, \cdots)\Psi_n(z)\cos\theta_2^{(0)}, \quad (3.17)$$

where $\theta_i^{(0)} \equiv kx + l_i y - \omega t + \phi_i(Y_2, \cdots)$, $i = 1, 2$. The BCs on A_i and ϕ_i, $i = 1, 2$ are at $Y_2 = 0$; that is, at $y = 0$: $A_1 = A_2 = A$ and $\phi_1 = \phi_2 = \phi$. The additional forcing terms on the rhs of (3.1) are

$$\begin{aligned} -2\partial_t\partial_{yY_2}\psi^{(0)} - \sin\alpha\partial_{Y_2}\psi^{(0)} &= -(2\omega l_1 + \sin\alpha)\Psi_n \\ &\times (\partial_{Y_2}A_1\cos\theta_1^{(0)} - A_1\partial_{Y_2}\phi_1\sin\theta_1^{(0)}) \\ &+ (2\omega l_2 + \sin\alpha)\Psi_n \\ &\times (\partial_{Y_2}A_2\cos\theta_2^{(0)} - A_2\partial_{Y_2}\phi_2\sin\theta_2^{(0)}). \end{aligned} \quad (3.18)$$

When (3.18) is multiplied by $\Psi_l(z)$ and depth integrated, its rhs is proportional to δ_{ln}. It is precisely for $l = n$ that we need these extra terms. We want to eliminate the secular terms from the rhs of (3.8) plus the depth integral of Ψ_l times the rhs of (3.18). The secular terms are removed by demanding that

$$\left.\begin{aligned} \partial_{Y_2}A_1 = \partial_{Y_2}A_2 &= 0 \\ (2\omega l_1 + \sin\alpha)A\partial_{Y_2}\phi_1 - \tfrac{1}{2}AkB_{12}C_n &= 0 \\ -(2\omega l_2 + \sin\alpha)A\partial_{Y_2}\phi_2 + \tfrac{1}{2}AkB_{12}C_n &= 0 \end{aligned}\right\}, \quad (3.19)$$

[1] What we actually mean by removing secular terms is that each forcing term that would otherwise produce a secular term is annihilated by choosing its coefficient to be zero.

which immediately implies using the BCs that $A_1 = A_2 = A$ [a constant at this order of approximation, but in general $A(Y_3, \cdots)$], and

$$\phi_i = \frac{(-1)^{i-1}kB_{12}C_n}{2\omega(l_1 - l_2)}Y_2 + \phi(Y_3, \cdots), \quad i = 1, 2. \quad (3.20)$$

Therefore, second-order nonlinear interactions change the *phase* of the waves but not their amplitude, in contrast to resonant interactions at first order, which change their amplitude but not their phase (GZ; Graef 1993). The linear growth in $\epsilon^2 y$ of the phases $\phi_{1,2}$ could also be interpreted as an $O(\epsilon^2)$ correction to the offshore wavenumbers $l_{1,2}$, respectively, so that now we could write $l_i + \epsilon^2 l_i^{(2)}$ with

$$l_i^{(2)} = (-1)^{i-1}\frac{kB_{12}C_n}{2\omega(l_1 - l_2)} = (-1)^i\frac{A^2k^2(l_1 - l_2)C_n\sin\alpha}{4\omega^2}, \quad i = 1, 2. \quad (3.21)$$

Thus, the effect of the steady flow plus transients on the incident–reflected RW field is to change their wavenumber normal to the wall, that is, $l_{1,2}$. Note that $\phi_1 + \phi_2 = 2\phi(Y_3, \cdots)$ but $\phi_1 - \phi_2 = kB_{12}C_nY_2/[\omega(l_1 - l_2)]$; this implies that only the steady part of the first-order solution needs to be modified (at second order).

It is easy to show that to $O(\epsilon^2 y)$, or in loose terms, close to the boundary,

$$\underbrace{\psi^{(0)}}_{\text{corrected}} \approx \underbrace{\psi^{(0)}}_{\text{uncorrected}} + \epsilon^2\Psi_n\underbrace{\Phi_n^{(2)}}_{(3.14)}, \quad (3.22)$$

indicating that the straightforward expansion is correct near the reflecting wall.

The change in the waves' phase is a general result for nonlinear wave–wave interactions at $O(\epsilon^2)$ whenever the dynamics has a quadratic nonlinearity. In Graef (1994), an example is worked out in a laterally unbounded ocean and taking $\psi^{(0)}$ as the superposition of two *arbitrary* RWs. At second order, multiple timescales lead to an $O(\epsilon^2)$ Doppler shift of the frequency of each wave, proportional to the amplitude squared of the other one.

c. Second-order solution

To minimize the amount of algebra, we will restrict the second-order solution to the barotropic case. The forcing for $\psi^{(2)}$ in the barotropic case is obtained putting $n = 0$ in the foregoing analysis and realizing that $J(\psi^{(0)}, -L^2f_0^2\lambda_0\psi^{(1)}) + J(\psi^{(1)}, -L^2f_0^2\lambda_0\psi^{(0)}) \equiv 0$. Since the form of $\psi_{\text{hom}}^{(1)}$ depended on the interval in which k lay [see (2.20)], we have to consider two different cases.

1) $\psi_{\text{hom}}^{(1)}$ OSCILLATORY: $k \in [k_-, k_+]$

The equation for $\psi^{(2)}$ is

$$\mathcal{M}_0[\psi^{(2)}] = -\frac{1}{2}AkB_{12}\{C_3\sin(2\theta_1^{(0)}-\theta_2^{(0)}) + C_4\sin(2\theta_2^{(0)}-\theta_1^{(0)}) + C_5[\sin(\theta_1^{(0)}+\theta_2^{(1)})+\sin(\theta_1^{(0)}-\theta_2^{(1)})] + C_6[\sin(\theta_2^{(0)}+\theta_2^{(1)})+\sin(\theta_2^{(0)}-\theta_2^{(1)})] + C_7\sin(2\theta_1^{(0)}+\theta_2^{(0)}) + C_8\sin(2\theta_2^{(0)}+\theta_1^{(0)})\}, \quad (3.23)$$

where $\mathcal{M}_0$ is the linear operator of the QGPVE in the barotropic case and the coefficients C_3 through C_8 are

$$C_{2+i} = (-1)^i\frac{\delta_{i1}l_2^2+\delta_{i2}l_1^2-2l_1l_2-k^2}{\sin\alpha}, \quad i=1,2 \quad (3.24)$$

$$C_{4+i} = (-1)^i\frac{\sin\alpha}{4\omega^2\lambda'}(\eta_2-2l_i)^2, \quad i=1,2 \quad (3.25)$$

$$C_{6+i} = \frac{(l_1-l_2)}{2\omega\lambda'}\left[(-1)^{i-1}\frac{\sin\alpha}{2\omega}(l_1-l_2)-\lambda'\right], \quad i=1,2, \quad (3.26)$$

in which $\lambda' \equiv \lambda - L^2f_0^2\lambda_0$. Note that the secular terms with coefficient C_0 do not appear in (3.23), since they have been eliminated using multiple scales, and we have omitted the subscript 0 (coming from $m=0$) in $\theta_2^{(1)}$ and η_2.

The procedure to solve (3.23) is the same as in section 2c: we find a particular solution to each forcing term and supplement it with a homogeneous solution to satisfy (3.2).

The final solution to the second-order problem is

$$\psi^{(2)} = \sum_{i=1}^{2}\Bigg[A_{2+i}^{(2)}\cos(2\theta_i^{(0)}-\delta_{i2}\theta_1^{(0)}-\delta_{i1}\theta_2^{(0)}) + A_{4+i,s}^{(2)}\cos(\theta_i^{(0)}+\theta_2^{(1)}) + A_{4+i,d}^{(2)}\cos(\theta_i^{(0)}-\theta_2^{(1)}) + A_{6+i}^{(2)}\cos(2\theta_i^{(0)}+\delta_{i2}\theta_1^{(0)}+\delta_{i1}\theta_2^{(0)}) - (A_{2+i}^{(2)}+A_{4+i,d}^{(2)})\cos\theta_2^{(0)} - (A_{4+i,s}^{(2)}+A_{6+i}^{(2)})\begin{Bmatrix}\cos\theta_2^{(2)}\\ e^{-\mu^{(i)}y}\cos\theta_r^{(2)}\end{Bmatrix}\Bigg], \quad (3.27)$$

where

$$\theta_2^{(2)} \equiv 3kx + \mu_2y - 3\omega t + 3\phi, \quad (3.28)$$

$$\theta_r^{(2)} \equiv 3kx + \mu^{(r)}y - 3\omega t + 3\phi, \quad (3.29)$$

in which the dispersion relation $3\omega = \sigma_0(3k, \mu)$ is satisfied, yielding

$$\mu_{1,2} = -\frac{\sin\alpha}{6\omega} \pm \left[\frac{1}{36\omega^2} - L^2f_0^2\lambda_0 - \left(3k+\frac{\cos\alpha}{6\omega}\right)^2\right]^{1/2}, \quad (3.30)$$

and the upper (lower) term within the large braces is taken if the roots $\mu_{1,2}$ are real (complex). If the roots are real, we choose μ_2 (negative radical) because it corresponds to the reflected RW; if they are complex we choose $\mu_1 = \mu^{(r)} + i\mu^{(i)}$, the exponentially decaying RW. In the rigid-lid case, $\mu_{1,2}$ are real if $k \in \frac{4}{9}[k_-, k_+]$. The amplitudes in (3.27) are, for $i = 1, 2$:

$$A_{2+i}^{(2)} = \frac{\frac{1}{2}AkB_{12}C_{2+i}}{[\omega-\sigma_0(k, 2l_i-\delta_{i2}l_1-\delta_{i1}l_2)] \times [k^2+(2l_i-\delta_{i2}l_1-\delta_{i1}l_2)^2+L^2f_0^2\lambda_0]} \quad (3.31)$$

$$A_{4+i,s}^{(2)} = \frac{\frac{1}{2}AkB_{12}C_{4+i}}{[3\omega-\sigma_0(3k, l_i+\eta_2)] \times [(3k)^2+(l_i+\eta_2)^2+L^2f_0^2\lambda_0]} \quad (3.32)$$

$$A_{4+i,d}^{(2)} = \frac{\frac{1}{2}AkB_{12}C_{4+i}}{[-\omega-\sigma_0(-k, l_i-\eta_2)] \times [(k)^2+(l_i-\eta_2)^2+L^2f_0^2\lambda_0]} \quad (3.33)$$

$$A_{6+i}^{(2)} = \frac{\frac{1}{2}AkB_{12}C_{6+i}}{[3\omega-\sigma_0(3k, 2l_i+\delta_{i2}l_1+\delta_{i1}l_2)] \times [(3k)^2+(2l_i+\delta_{i2}l_1+\delta_{i1}l_2)^2+L^2f_0^2\lambda_0]}. \quad (3.34)$$

We examined whether the amplitudes in (3.27) become infinite. Their numerators [e.g., see (3.34) and (3.26)] are bounded if $|\sin\alpha| > 1/3$, for this implies that $\lambda' \neq 0$ for k real. If their denominators vanish, we have resonance. In all four possible cases of second-order resonance, one can arrive at an equation $\mathcal{G}(k, \omega) = 0$, relating k and ω. Thus, there is only one free parameter left. For example, in the case $\omega = \sigma_0(k, \eta_2 - l_i)$, we also have $\omega = \sigma_0(k, l_i)$ and $2\omega = \sigma_0(2k, \eta_2)$; that is, three equations and four parameters: ω, k, l_i, and η_2. We found that $A_{2+i}^{(2)}$ is bounded, $A_{6+i}^{(2)}$ is bounded if $l_i\eta_2 \geq 0$ and $|\sin\alpha| > 1/3$, $A_{4+i,d}^{(2)}$ is bounded if $|\sin\alpha| > 1/3$, and $A_{6+i}^{(2)}$ is bounded if $(-1)^{i-1}\sin\alpha \leq 0$ and $|\sin\alpha| > 1/3$. These are sufficient conditions preventing resonance.

2) $\psi_{\rm hom}^{(1)}$ EXPONENTIALLY DECAYING: $k \notin [k_-, k_+]$

The PDE to be solved is

$$\mathcal{M}_0[\psi^{(2)}] = -\frac{1}{2}AkB_{12}\{C_3\sin(2\theta_1^{(0)} - \theta_2^{(0)}) + C_4\sin(2\theta_2^{(0)} - \theta_1^{(0)}) + e^{-\eta^{(i)}y} \times (C_5[\sin(\theta_1^{(0)} + \theta_r^{(1)}) + \sin(\theta_1^{(0)} - \theta_r^{(1)})] + C_6[\sin(\theta_2^{(0)} + \theta_r^{(1)}) + \sin(\theta_2^{(0)} - \theta_r^{(1)})]) + C_7\sin(2\theta_1^{(0)} + \theta_2^{(0)}) + C_8\sin(2\theta_2^{(0)} + \theta_1^{(0)}) + e^{-\eta^{(i)}y}(C_9[\cos(\theta_1^{(0)} - \theta_r^{(1)}) - \cos(\theta_1^{(0)} + \theta_r^{(1)})] + C_{10}[\cos(\theta_2^{(0)} - \theta_r^{(1)}) - \cos(\theta_2^{(0)} + \theta_r^{(1)})])\}, \quad (3.35)$$

where $C_{3,4,7,8}$ are given exactly as in (3.24) and (3.26) and $C_{5,6,9,10}$ are given by

$$C_{4+i} = (-1)^i\frac{\sin\alpha}{4\omega^2\lambda'}[(\eta^{(r)} - 2l_i)^2 - \eta^{(i)2}], \quad i = 1, 2 \quad (3.36)$$

$$C_{8+i} = (-1)^i\frac{\sin\alpha}{2\omega^2\lambda'}\eta^{(i)}(2l_i - \eta^{(r)}), \quad i = 1, 2. \quad (3.37)$$

Again, we have omitted the subscript 0 (coming from $m = 0$) in $\theta_r^{(1)}$, $\eta^{(r)}$, and $\eta^{(i)}$.

The final solution to the second-order problem for $k \in [k_-, k_+]^c \cap (k_2, k_1)$, where $[k_-, k_+]^c$ is the complement of $[k_-, k_+]$ and (k_2, k_1) is the interval[2] in which $l_{1,2}$ are real and different, is

$$\psi^{(2)} = \sum_{i=1}^{2}[A_{2+i}^{(2)}\cos(2\theta_i^{(0)} - \delta_{i2}\theta_1^{(0)} - \delta_{i1}\theta_2^{(0)}) + e^{-\eta^{(i)}y} \times \{A_{4+i,s}^{(2)}\sin(\theta_i^{(0)} + \theta_r^{(1)}) + A_{4+i,d}^{(2)}\sin(\theta_i^{(0)} - \theta_r^{(1)}) + A_{8+i,s}^{(2)}\cos(\theta_i^{(0)} + \theta_r^{(1)}) + A_{8+i,d}^{(2)}\cos(\theta_i^{(0)} - \theta_r^{(1)})\} + A_{6+i}^{(2)}\cos(2\theta_i^{(0)} + \delta_{i2}\theta_1^{(0)} + \delta_{i1}\theta_2^{(0)}) - (A_{2+i}^{(2)} + A_{8+i,d}^{(2)})\cos\theta_2^{(0)} - A_{4+i,s}^{(2)}e^{-\mu^{(i)}y}\sin\theta_r^{(2)} + A_{4+i,d}^{(2)}\sin\theta_2^{(0)} - (A_{6+i}^{(2)} + A_{8+i,s}^{(2)})e^{-\mu^{(i)}y}\cos\theta_r^{(2)}], \quad (3.38)$$

where $A_{2+i}^{(2)}$ and $A_{6+i}^{(2)}$ are given in (3.31) and (3.34), and the rest of the amplitudes are, for $i = 1, 2$:

$$A_{4+i,s}^{(2)} = \frac{\frac{1}{2}AkB_{12}(C_{8+i}d_i - C_{4+i}f_i)}{d_i^2 + f_i^2} \quad (3.39)$$

$$A_{8+i,s}^{(2)} = \frac{\frac{1}{2}AkB_{12}(C_{4+i}d_i + C_{8+i}f_i)}{d_i^2 + f_i^2} \quad (3.40)$$

$$A_{4+i,d}^{(2)} = \frac{-\frac{1}{2}AkB_{12}(C_{8+i}g_i + C_{4+i}h_i)}{g_i^2 + h_i^2} \quad (3.41)$$

$$A_{8+i,d}^{(2)} = \frac{\frac{1}{2}AkB_{12}(C_{4+i}g_i - C_{8+i}h_i)}{g_i^2 + h_i^2}, \quad (3.42)$$

where in turn

$$\left.\begin{aligned} d_i &= [3\omega - \sigma_0(3k, l_i + \eta^{(r)})] \times [(3k)^2 + (l_i + \eta^{(r)})^2 + L^2f_0^2\lambda_0] - 3\omega\eta^{(i)2} \\ f_i &= \eta^{(i)}[-6\omega(l_i + \eta^{(r)}) - \sin\alpha] \\ g_i &= -[\omega - \sigma_0(k, \eta^{(r)} - l_i)] \times [k^2 + (\eta^{(r)} - l_i)^2 + L^2f_0^2\lambda_0] + \omega\eta^{(i)2} \\ h_i &= \eta^{(i)}[2\omega(l_i - \eta^{(r)}) - \sin\alpha]. \end{aligned}\right\} \quad (3.43)$$

It can easily be shown that if η is complex, then μ is complex. This is the reason why only the trapped RW $\sim e^{-\mu^{(i)}y}$ appears in the last term of (3.38). Note that this case 2 reduces to case 1, where $\psi_{\text{hom}}^{(1)}$ is oscillatory in y, by putting $\eta^{(i)} = 0$, $\eta^{(r)} = \eta_2$, and $\theta_r^{(1)} = \theta_2^{(1)}$. In case 1, if μ is real, we put $\mu^{(i)} = 0$, $\mu^{(r)} = \mu_2$, and $\theta_r^{(2)} = \theta_2^{(2)}$. Indeed, we can see that if $\eta^{(i)} = 0$, then $A_{4+i,s}^{(2)} = A_{4+i,d}^{(2)} = 0$ and $A_{8+i,s/d}^{(2)}$ of case 2 becomes $A_{4+i,s/d}^{(2)}$ of case 1.

Finally, we show that the denominators of the amplitudes defined in (3.39)–(3.42) cannot vanish. If $\eta^{(i)} \neq 0$ then $f_i = 0 \Leftrightarrow l_i + \eta^{(r)} = -\sin\alpha/(6\omega)$, which when substituted into d_i results in $d_i = 15\omega k^2 + \frac{5}{48}\sin^2\alpha/\omega > 0$, since we have assumed $k \neq 0$ and $\sin\alpha \neq 0$ (see page 1869). In exactly the same fashion one shows that for $\eta^{(i)} \neq 0$, $h_i = 0$ implies $g_i = 3\omega k^2 + \frac{3}{16}\sin^2\alpha/\omega > 0$. Therefore, the amplitudes in (3.38) that have the $e^{-\eta^{(i)}y}$ factor remain bounded if $|\sin\alpha| > 1/3$.

4. Third-order problem

The main reason why we go to third-order is the realization that the forcing at $O(\epsilon^3)$ contains steady and x-independent terms, whose response contributes to the steady flow found at first order. The steady flow at $O(\epsilon^3)$ is the next higher order correction to the MM flow; the x average (or time average) of the second-order flow is zero.

[2] Given by $(k_2, k_1) = (-\cos\alpha/(2\omega) - R_0, -\cos\alpha/(2\omega) + R_0)$, where $R_0 = [1/(4\omega^2) - L^2f_0^2\lambda_0]^{1/2}$.

Although one may argue with reason that if $\epsilon \ll 1$ then an $O(\epsilon^3)$ correction is too small to really care for, this might not be true in the reflection problem. In fact, the third-order correction to the MM steady flow is not negligible at all for cases in which the perturbative solution is still valid, as shown in section 5.

We shall restrict the third-order problem to the barotropic case, to minimize (?) the amount of algebra, and anticipating that we will have forcing functions that produce secular terms in $\psi^{(3)}$, we include the additional terms in the forcing that arise because of the multiple space scales (section 3b). Noting that $J(\psi^{(0)}, -L^2 f_0^2 \lambda_0 \psi^{(2)}) + J(\psi^{(2)}, -L^2 f_0^2 \lambda_0 \psi^{(0)}) \equiv 0$ and $J(\psi^{(1)}, -L^2 f_0^2 \lambda_0 \psi^{(1)}) \equiv 0$, the third-order barotropic problem is

$$\begin{aligned}\mathcal{M}_0[\psi^{(3)}] = &-J(\psi^{(0)}, \nabla^2\psi^{(2)}) - J(\psi^{(1)}, \nabla^2\psi^{(1)}) \\ &- J(\psi^{(2)}, \nabla^2\psi^{(0)}) - (\partial_x\psi^{(0)})\partial_{Y_2}\nabla^2\psi^{(0)} \\ &+ (\partial_{Y_2}\psi^{(0)})\partial_x\nabla^2\psi^{(0)} - 2[(\partial_x\psi^{(0)})\partial_y\partial_{yY_2}\psi^{(0)} \\ &- (\partial_y\psi^{(0)})\partial_x\partial_{yY_2}\psi^{(0)}] - 2\partial_t(\partial_{yY_3}\psi^{(0)} + \partial_{yY_2}\psi^{(1)}) \\ &- \sin\alpha(\partial_{Y_3}\psi^{(0)} + \partial_{Y_2}\psi^{(1)}) \quad (4.1)\end{aligned}$$

$$\partial_x\psi^{(3)} = 0 \quad \text{at} \quad y = 0 \qquad (4.2)$$

$$\psi^{(3)} \quad \text{bounded as} \quad x \to \pm\infty, y \to \infty. \qquad (4.3)$$

In (4.1), the Jacobians indicated by J, the Laplacian operator and the spatial derivatives in the $\mathcal{M}_0$ operator imply differentiation with respect to x and y. The derivatives with respect to the longer space scales Y_2 and $Y_3 = \epsilon^3 y$ are explicitly indicated. The calculation of the forcing for $\psi^{(3)}$ is done in the appendix.

The corrections to the steady flow of MM

To get the *steady* response at $O(\epsilon^3)$, we consider only the steady forcing in (A.21). If we are interested only in the steady current $u_s^{(3)}$ and not in the corresponding streamfunction, we do not have to solve anything, since the steady streamfunction satisfies

$$\sin\alpha\partial_y\psi_s^{(3)} = \text{steady forcing on the rhs of (A.21)}, \qquad (4.4)$$

and $u_s^{(3)} = -\partial_y\psi_s^{(3)}$. Therefore, the $O(\epsilon^3)$ correction to the steady flow parallel to the wall is

$$\begin{aligned}u_s^{(3)}(y) = -\frac{1}{\sin\alpha}\Bigg\langle &\left[-\frac{1}{2}Ak(C_{31} + C_{42} + H_{11} + H_{21}) - B_{12}^{(2)} + \frac{kB_{12}^2C_0}{\omega(l_1 - l_2)^2}\right]\cos(\theta_1^{(0)} - \theta_2^{(0)}) \\ &- \frac{1}{2}Ak[(H_{5,d,1} + H_{6,d,1})\sin(\theta_1^{(0)} - \theta_2^{(0)}) + (C_{32} + C_{41})\cos2(\theta_1^{(0)} - \theta_2^{(0)})] \\ &+ e^{-\eta^{(i)}y}\Bigg\{\left[\frac{1}{2}Ak(C_{5,d,2} + C_{6,d,1}) - \frac{B_{12}^2k}{2\omega\lambda'}G_3\right]\cos(\theta_1^{(0)} + \theta_2^{(0)} - \theta_r^{(1)}) \\ &- \left[\frac{1}{2}Ak(S_{5,d,2} + S_{6,d,1}) - \frac{B_{12}^2k}{2\omega\lambda'}G_4\right]\sin(\theta_1^{(0)} + \theta_2^{(0)} - \theta_r^{(1)}) \\ &+ \frac{1}{2}Ak[C_{5,d,1}\cos(2\theta_1^{(0)} - \theta_r^{(1)}) + C_{6,d,2}\cos(2\theta_2^{(0)} - \theta_r^{(1)}) - S_{5,d,1}\sin(2\theta_1^{(0)} - \theta_r^{(1)}) \\ &- S_{6,d,2}\sin(2\theta_2^{(0)} - \theta_r^{(1)})]\Bigg\} - G_6e^{-2\eta^{(i)}y}\Bigg\rangle. \qquad (4.5)\end{aligned}$$

The coefficients $C_{2+i,j}$ (e.g., C_{31}), H_{ij}, $\cdots$, $i, j = 1, 2$ are defined in the appendix. Recall that the case η real is recovered in (4.5) if we put $\eta^{(i)} = 0$, $\eta^{(r)} = \eta_2$, and $\theta_r^{(1)} = \theta_2^{(1)}$.

The flow given by (4.5) is the modification to the steady flow found by MM (in the absence of dissipation) due to higher-order nonlinearities. In dimensional units, it is simply $u_{s*}^{(3)} = U\epsilon^3u_s^{(3)}$. Note that $u_s^{(3)}$ is *not,* in general, a periodic function of y (in case η real, $u_s^{(3)}$ would be periodic if the ratios of its wavenumbers were rational numbers). We have analyzed whether the amplitudes of the terms in $u_s^{(3)}$ could blow up through first- or second-order resonances. Our main result, supported by the analysis of section 3c, is that if $|\sin\alpha| > 1/3$ then $u_s^{(3)}$ is bounded.

If we did a time average over a wave period (or x average over a length $2\pi/|k|$) of $\psi^{(0)} + \epsilon\psi^{(1)} + \epsilon^2\psi^{(2)} + \epsilon^3\psi^{(3)}$ everything vanishes except $\epsilon\psi_{p1}^{(1)} + \epsilon^3\psi_s^{(3)}$, which is the steady circulation induced by the nonlinear interactions in the reflection of RWs.

5. Numerical applications

For numerical applications, the wave parameters n, ω, and k are chosen, *in that order,* such that $l_{1,2}$ is real and different. The wave amplitude A_* is determined using one of the following two methods.

1) The dimensional amplitude of the O(1) pressure is $P_*(z) = \rho_s f_0 A_* \Psi_n(z)$, where ρ_s is a reference density. At the sea surface we can write $P_*|_0 = \rho_s g a$, where g is the acceleration of gravity and a is the amplitude of

the sea surface elevation associated with the RWs. Then, for given a,

$$A_* = \frac{ga}{f_0 \Psi_n(0)}. \quad (5.1)$$

We can choose $A = 1$ so $\psi^{(0)} \sim O(1)$ and $A_* = UL$ [see text following (2.14)]. Note that A_* is independent of the RW's wavelength.

2) Choose $U_{\rm inc}$ to be the maximum horizontal speed of the incident wave field at $z = 0$. Then

$$A_* = \frac{U_{\rm inc}}{|\vec{k}_{\rm inc*}| \Psi_n(0)}, \quad (5.2)$$

where $\vec{k}_{\rm inc*}$ is the dimensional wavenumber vector of the incident wave. Thus, the wave amplitude depends linearly on the incident wave's wavelength. Again, $U = A_*/L(A = 1)$.

In the dimensionalization of $u_s^{(1)}$ the L drop out, so the choice of L is irrelevant; what matters is the value of A_* and the wave parameters k_* and $l_{1,2*}$ involved in B_{12*}. In other words, how L is chosen is arbitrary, but once we do choose an L, U must be computed from $U = A_*/L$ and ϵ from $\epsilon = U/(\beta L^2) = A_*/(\beta L^3)$ in the dimensionalization. The actual numerical value of $\epsilon = U/(\beta L^2)$ is then also irrelevant. Perhaps a better measure of the nonlinearity is

$$\epsilon_{\rm est} = \frac{\text{amplitude of } J_*(\psi_*^{(0)}, \nabla_*^2 \psi_*^{(0)})}{\text{amplitude (maximum) of } \beta(\cos\alpha\partial_{x_*}\psi_*^{(0)} + \sin\alpha\partial_{y_*}\psi_*^{(0)})}$$
$$= \frac{|B_{12*}|\Psi_n^2(0)}{\beta \max_{i=1,2}|(k_* \cos\alpha + l_{i*} \sin\alpha)| \times A_* \Psi_n(0)}. \quad (5.3)$$

To $O(\epsilon)$, the strength of the nonlinear terms is estimated by $\epsilon_{\rm est}$, which compares the amplitude of the nonlinear *forcing* with the amplitude of the linear terms. Given the complete $\psi^{(1)}$, we can check the validity of our perturbative solution by dividing the maximum amplitude of all the components of $\epsilon\psi^{(1)}$ by the amplitude of $\psi^{(0)}$. This ratio, $\epsilon_{\rm true}$, should be smaller than one, since otherwise the first-order correction is as large or larger than the leading order term. For example, in the barotropic case

$$\epsilon_{\rm true} = \epsilon \max\{|b_0/(\lambda - L^2 f_0^2 \lambda_0)|, |B_{12}/[(l_1 - l_2)\sin\alpha]|\}/A. \quad (5.4)$$

Nonetheless, $\epsilon_{\rm true}$ could have the disadvantage of underestimating (or overestimating) the size of the first-order correction if there is constructive (destructive) interference of the $\psi^{(1)}$ components.

The perturbative solution up to third order is periodic in time with frequency ω. The z dependence is given in terms of vertical normal modes that depend on $N(z)$. Thus, the solution is shown by plotting maps of the streamfunction as a function of x and y at $z = t = 0$. A single number that compares the size of the ith-order correction to the size of the jth-order solution is the ratio of their root mean squares; that is,

$$r_{i,j} = \frac{\text{rms}(\epsilon^i \psi^{(i)})}{\text{rms}(\epsilon^j \psi^{(j)})} = \frac{\sqrt{\sum_{x,y} (\epsilon^i \psi^{(i)})^2}}{\sqrt{\sum_{x,y} (\epsilon^j \psi^{(j)})^2}}. \quad (5.5)$$

The size of the second-order correction relative to the solution up to first order can be obtained from $r_{2,01} = \text{rms}(\epsilon^2 \psi^{(2)})/\text{rms}(\psi^{(0)} + \epsilon\psi^{(1)})$.

a. Observational evidence

Oh and Magaard (1984), MM, and Sun et al. (1988) compared the theoretically predicted steady current with geostrophic currents derived from "synoptic" observations along isolated sections more or less orthogonal to the Hawaiian Ridge. The available data did not allow an averaging along the ridge or a time averaging, but the authors justified that such comparisons were meaningful because the steady current was an order of magnitude larger than the currents associated with the Rossby waves.

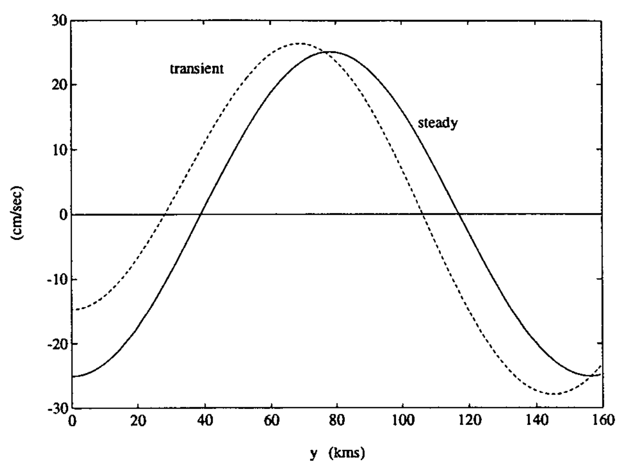

FIG. 1. Comparison between the steady (solid line) and the transient (dashed line) flow at $z = 0$: the steady flow and the velocity component parallel to the wall of the transients; that is, $u_t^{(1)} = -\partial_y(\psi_{\rm hom}^{(1)} + \psi_{p2}^{(1)})$ (dimensionalized) at $x = t = 0$, as a function of y_*. Note that they are of the same order of magnitude. Parameters: reference latitude $\theta_0 = 25°$, wall orientation $\alpha = 25°$ (measured clockwise from eastern direction), vertical mode number of incident–reflected RW pair $n = 0$, depth $H = 4500$ m (free surface), period $T = 1$ yr, wavenumber parallel to the wall $k_* = 0.001$ km^{-1}, angle between $\vec{k}_{\rm inc}$ and east $\theta_{\rm inc} = 268.6°$, maximum horizontal speed of incident wave field $U_{\rm inc} = 2$ cm s^{-1}, maximum horizontal speed of reflected wave field $U_{\rm ref} = 33.4$ cm s^{-1}, incident wave's wavelength $\Lambda_{\rm inc} = 2516$ km, reflected wave's wavelength $\Lambda_{\rm ref} = 151$ km, angle between the group velocity of incident wave and east $\phi_{\rm inc} = 177.3°$, $\epsilon_{\rm est} = 0.79$, $\epsilon_{\rm true} = 0.79$, $\max(\epsilon_{\rm inc}, \epsilon_{\rm ref}) = \max(U_{\rm inc}|\vec{k}_{\rm inc*}|^2/\beta, U_{\rm ref}|\vec{k}_{\rm ref*}|^2/\beta) = 28$.

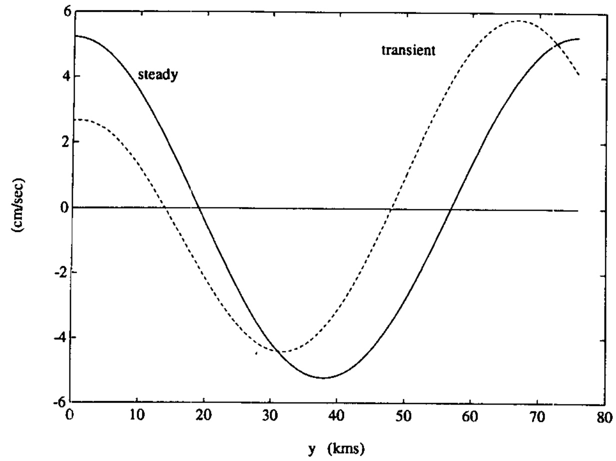

FIG. 2. As in Fig. 1 but for $\theta_0 = 35°$, $\alpha = 90°$, $n = 1$, $H = 4500$ m, stability period $T_N = 40$ min, $\theta_{inc} = 170°$, $U_{inc} = 1$ cm s^{-1}, $U_{ref} = 15.5$ cm s^{-1}, $\Lambda_{inc} = 1098$ km, $\Lambda_{ref} = 71$ km, $\phi_{inc} = 181.4°$, $\epsilon_{est} = 0.34$, $\epsilon_{true} = 0.36$, and $\max(\epsilon_{inc}, \epsilon_{ref}) = 46$.

The 2ω transients, however, were not studied. The steady flow and the x velocity component of the transients (at a particular x and t, since the transients are x and t dependent) are plotted as a function of the offshore coordinate for two different cases (Figs. 1 and 2). The boundary orientation in Fig. 1 has $\alpha = 25°$, the value used by MM for the Hawaiian Ridge. Both figures show clearly that the transient flow parallel to the wall is of the *same* order of magnitude as the steady flow. This is generally true, but one can imagine cases—for example, making λ "large"—in which the transients are much smaller than the steady flow.

What this means is that the transient flow superimposed on the steady flow will depend on *where* one measures along the boundary and *when* (disregarding the relatively weak contribution from the driving RWs—again, this is not always true). Assuming that the reflection of RWs is the only physical process that takes place along the northern side of the Hawaiian Ridge, the observed currents parallel to the ridge will not be the MM flow alone, but an MM flow highly contaminated by the transients. It is then not surprising that in some instances there was little resemblance between the MM flow and the observations. A fair comparison between the theoretically predicted mean current and observations would require data that allow an x or time averaging to remove the transients and the incident–reflected waves.

In the mean time, observations pertaining to this paper have been made in the Hawaii Ocean Time-Series (HOT) project (Chiswell and Lukas 1990; Chiswell et al. 1990; Winn et al. 1992; Winn et al. 1993). In that project, time-series cruises have been made since 1988 on approximately monthly intervals between two stations: the ALOHA station located at 22° 45′N, 158°W is about 100 km north of Kahuku Point, Oahu, Hawaii, and the Kahe Point station located at 21° 20.6′N, 158° 16.4′W near Kahe Point, Oahu, Hawaii (Fig. 3). Current measurements are made on HOT

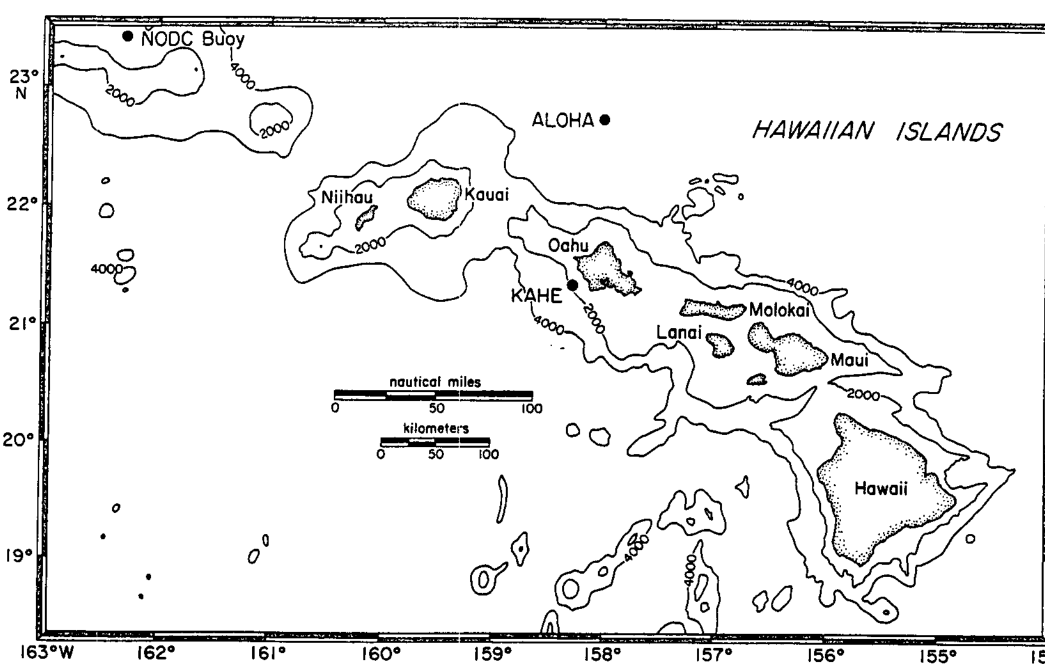

FIG. 3. Locations of station ALOHA and Kahe Point Station (from Karl and Winn 1991).

cruises using a shipboard Acoustic Doppler Current Profiler (ADCP) when a ship with the necessary equipment is available for monthly cruises. In addition, lowered ADCP measurements have been made on several HOT cruises (Chiswell et al. 1990).

Preliminary results from the current measurements have been made available to us by E. Firing (1993, personal communication). Figure 4 shows the profile of currents along the Kahe Point–ALOHA station course averaged over a depth range from 20 to 50 m and over an observational period from October 1988 through January 1993. This current profile shows significant resemblance to the current (North Hawaiian Ridge Current) predicted by MM and Oh and Magaard (1984) and later studied by Sun et al. (1988) based on two hydrographic sections. The HOT dataset is, of course, far superior for the study of the current than the data used by Sun et al. (1988), and we consider the results of the HOT current measurements as the first significant evidence that the North Hawaiian Ridge Current may actually exist. According to E. Firing (1993, personal communication), the currents measured in the HOT project have the following additional features: Their strength decreases with depth but their direction remains largely unchanged. They do not show a strong annual cycle, but they do show strong interannual fluctuations. Annually averaged currents maintain their basic westward direction with a small deviation to the north; their direction is never reversed. Standard deviations of the measured currents are of the same order of magnitude as the maximum mean values. As mentioned above, much of the variability occurs at interannual frequencies. But significant variability also occurs at timescales smaller than a year.

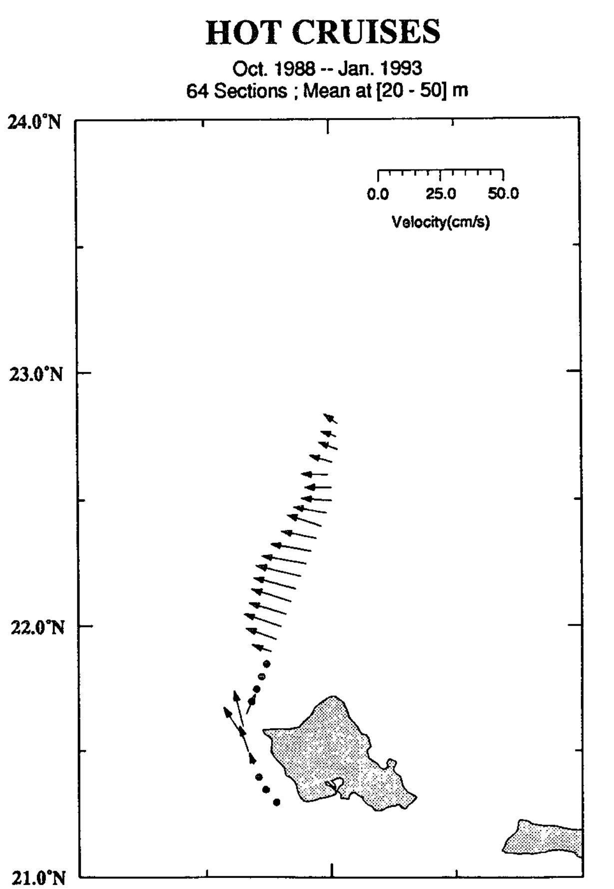

FIG. 4. Mean currents north of Oahu, Hawaii, averaged over a depth range from 20–50 m and over a period from October 1988 through January 1993 (from E. Firing 1993, personal communication).

b. Characteristics of solution in parameter space

One of the main advantages of an analytical solution (versus a numerical one, for example) is that it is relatively easy to explore its behavior in parameter space. For instance, one can compute the correction to the offshore wavenumbers (section 3b) as a function of different wave parameters without actually computing the solution.

If the correction to a quantity τ is $\delta\tau$, the size of the correction in % is $100|\delta\tau/\tau|$. The shift in $l_{1,2}$ leads to a correction of the wavelengths $\Lambda_{\rm inc}$ and $\Lambda_{\rm ref}$ whose size is given by $100|\Lambda(l_i + \epsilon^2 l_i^{(2)}) - \Lambda(l_i)|/\Lambda(l_i)$, $i = 1$ and $i = 2$, respectively. The correction to the wavenumber of the steady flow is $100\epsilon^2|l_1^{(2)} - l_2^{(2)}|/(l_1 - l_2) = 100\epsilon^2 A^2 k^2 |C_n \sin\alpha|/(2\omega^2)$. These corrections and other parameters are plotted in Figs. 5–7 as functions of $\Lambda_{\rm inc}$ and the angle between $\vec{k}_{\rm inc}$ and east, $\theta_{\rm inc}$, for three cases.

The first case (Fig. 5) has $U_{\rm inc} \sim O(1)$ cm s^{-1} for all waves and $U_{\rm ref} < 20$ cm s^{-1} for waves with periods less than 2 years. Note that $\epsilon_{\rm est}$ and $\epsilon_{\rm true}$ are very similar; this is perhaps not surprising since the problem for $\psi^{(1)}$ is linear (as for all orders). As expected, there is good correlation between $\epsilon_{\rm est}$ and the amplitude of $u_{s*}^{(1)}$. For $\epsilon_{\rm est} < 0.7$ the corrections to $l_1 - l_2$, $\Lambda_{\rm inc}$, and $\Lambda_{\rm ref}$ are less than 20%, 30%, and 15%. (It would be less than 5% if it were not for the lower-left corner maximum.) The correction is always larger in the long RW for all boundaries, because $l_1^{(2)} = -l_2^{(2)}$. The largest corrections are for incident RWs with $\theta_{\rm inc} < 125°$ and $\theta_{\rm inc} > 250°$. In general, the more meridionally oriented the incident wave vector is, the more nonlinear the problem becomes (see also Figs. 6–7).

In Fig. 6, $\theta_{\rm inc} < 165°$ since for $165° < \theta_{\rm inc} < 260°$ the incident wavelengths would exceed 3000 km, and we consider only incident RWs with $\Lambda_{\rm inc} \in [100$ km, 3000 km$]$. Here, $\epsilon_{\rm est} < \epsilon_{\rm true}$ in all the domain, but with similar values; $\epsilon_{\rm ref} = U_{\rm ref}|\vec{k}_{\rm ref*}|^2/\beta$ (not shown) is an order of magnitude larger than $\epsilon_{\rm est}$, indicating that al-

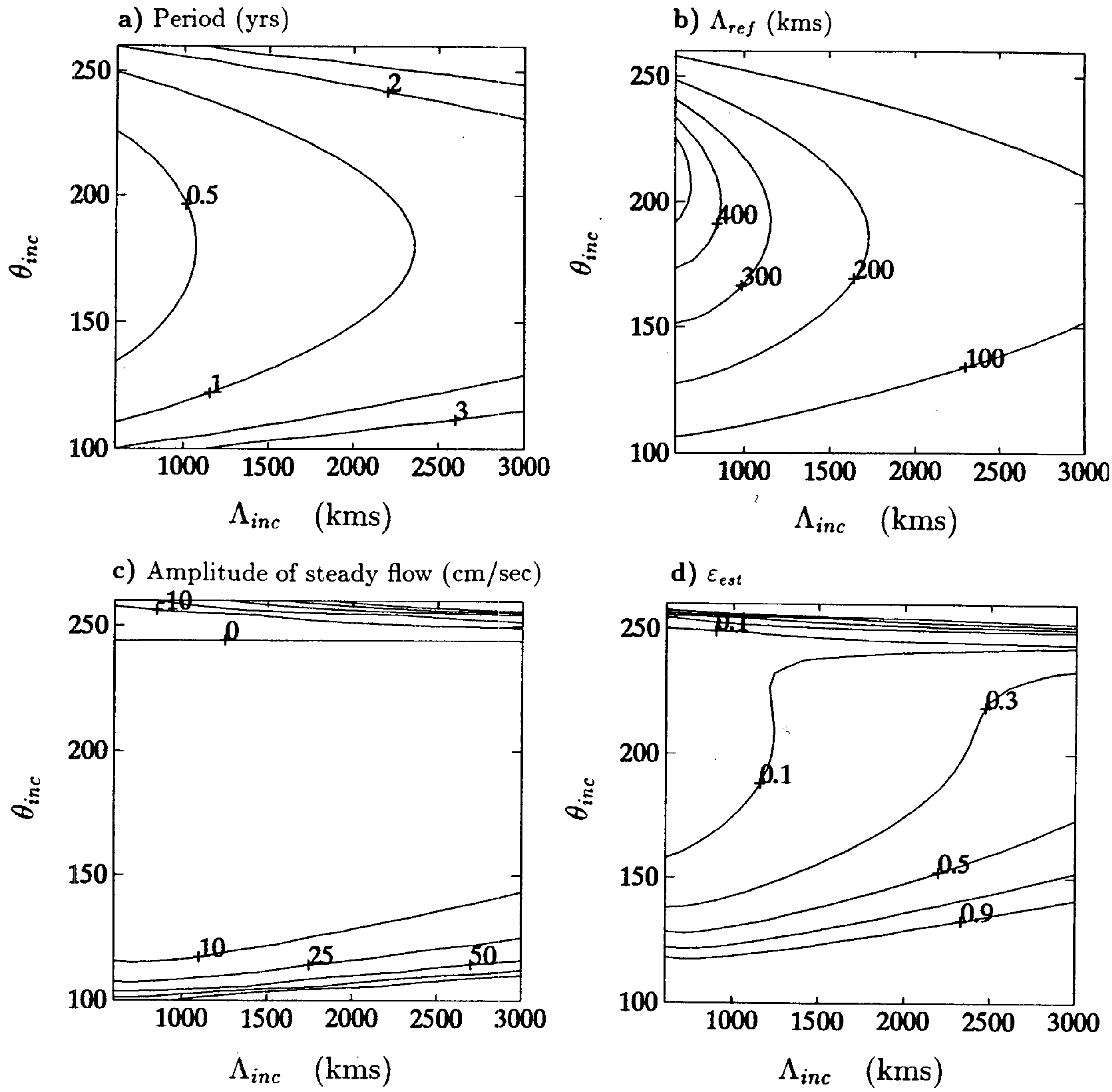

FIG. 5. Maps of (a) wave period T in years; (b) Λ_{ref} in km; (c) amplitude of the steady flow at $z = 0$, $B_{12*}\Psi_n^2(0)/(\beta \sin\alpha)$, in cm s^{-1}; (d) ϵ_{est}; (e) ϵ_{true}; (f) the correction in % to $l_1 - l_2$; (g) the correction in % to Λ_{inc}; and (h) the correction in % to Λ_{ref} as functions of (Λ_{inc}, θ_{inc}). The domain is (600 km, 3000 km) × (100°, 260°). (The offshore component of the group velocity is negative, that is, incident, for

though the reflected waves might be highly nonlinear, this is not necessarily true for the reflection problem. The tendency for the amplitude of the steady flow, the ϵ's, and for the corrections to be smaller for larger Λ_{inc} is a consequence of both $A_* \sim \Lambda_{inc}^{-1}$ and the increase of ω with Λ_{inc}. The upper left of the corrections maps (Figs. 6f–h) shows large values, especially that of $l_1 - l_2$, whereas the same region of the amplitude of $u_{s*}^{(1)}$, ϵ_{est}, and ϵ_{true} maps (Figs. 6c–e) shows small values. This is attributable to a relative maximum of C_n there. A case with $\theta_{inc} = 160°$ and $T = 0.3$ years, a point in such a region, yields $r_{1,0} = 0.43$, $r_{2,0} = 2.31$, and $r_{2,01} = 2.13$, which shows that the perturbative solution is not valid even though ϵ_{est} and ϵ_{true} are small. What we learn from this is that the smallness of ϵ_{est} and ϵ_{true} is not sufficient for the perturbation expansion to be valid. The problem with annual period waves is strongly nonlinear (ϵ_{est}, ϵ_{true}) > 2), but it is possible still to find

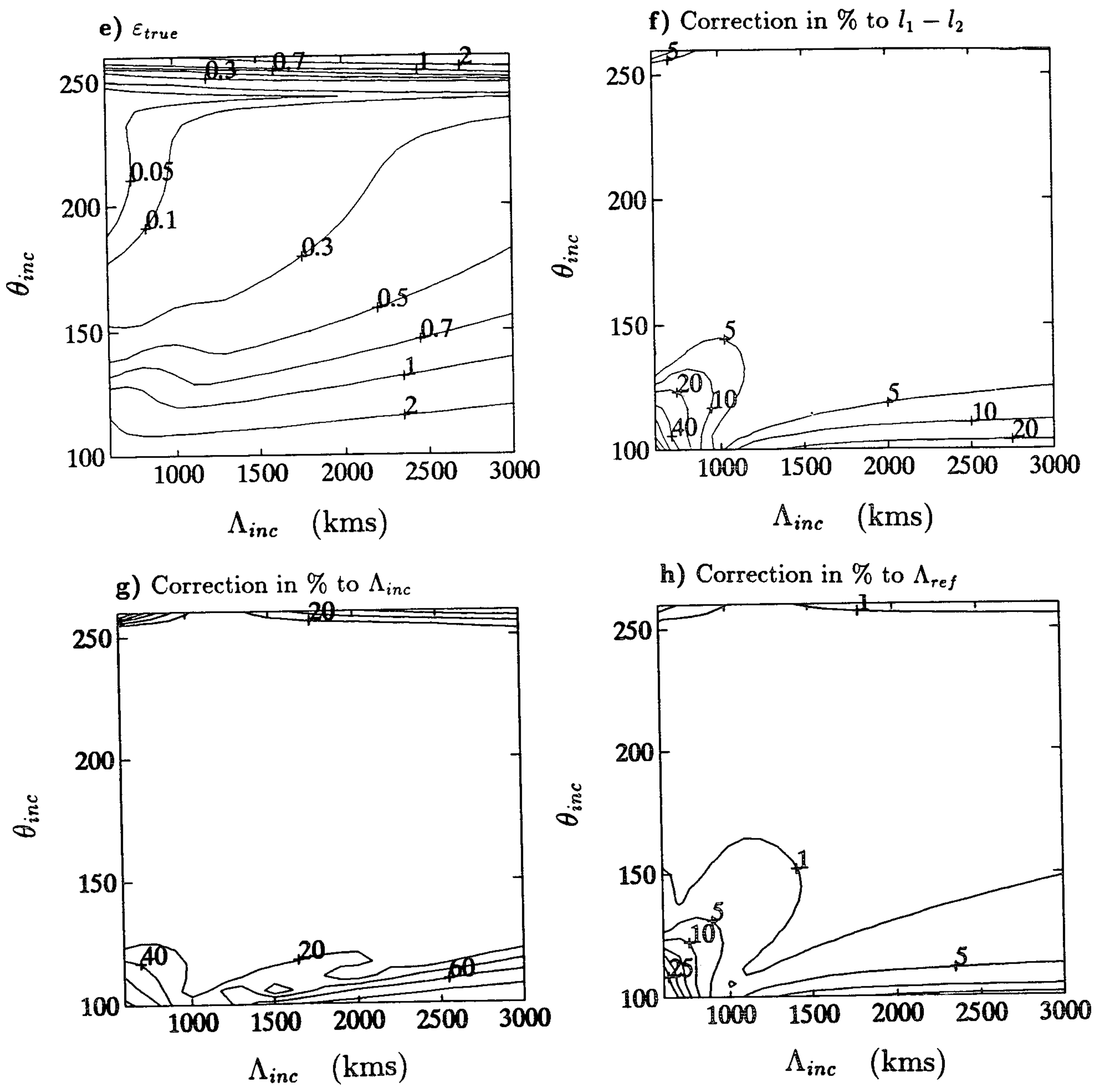

FIG. 5. (*Continued*) all waves defined in the region.) Parameters: $\theta_0 = 25°$, $\alpha = 25°$, $n = 1$, $H = 4500$ m, $T_N = 40$ min. Wave amplitudes calculated from $a = 1$ cm. The zero contour line in the amplitude of $u_{s*}^{(1)}$ is for $\theta_{inc} = 245° = 270° - \alpha$ and corresponds to waves with $k = 0$. See Fig. 1 for meaning of symbols.

moderately nonlinear cases with ϵ_{est}, $\epsilon_{true} < 1$, and most importantly $r_{1,0}$, $r_{2,0}$, and $r_{2,01} < 1$, by putting $U_{inc} = 2$ cm s^{-1} (see Figs. 1 and 8).

Finally, the typical case (Fig. 7) of a meridional midlatitude western boundary with first mode baroclinic RWs, with the wave amplitude chosen from $U_{inc} = 1$ cm s^{-1}, is clearly more strongly nonlinear than the case in Fig. 5; the region in (Λ_{inc}, θ_{inc})-space where $\epsilon_{est} < 1$ is reduced. But interestingly enough, the corrections to $l_1 - l_2$, Λ_{inc}, and Λ_{ref} are less than 5%, 30%, and 5% in that region. Note that there is no apparent difference between ϵ_{est} and ϵ_{true}.

c. Examples of the solution

The horizontal domain of the maps has x spanning a distance along the wall from $-\pi/|k_*|$ to $\pi/|k_*|$, so the pattern shown repeats itself in the x direction (along the wall). The range in the offshore direction was chosen from $y = 0$ (the wall) to $y_* = 2\pi/\min(|l_{1*} + l_{2*}|, l_{1*} - l_{2*})$. The field variables are, in general, not pe-

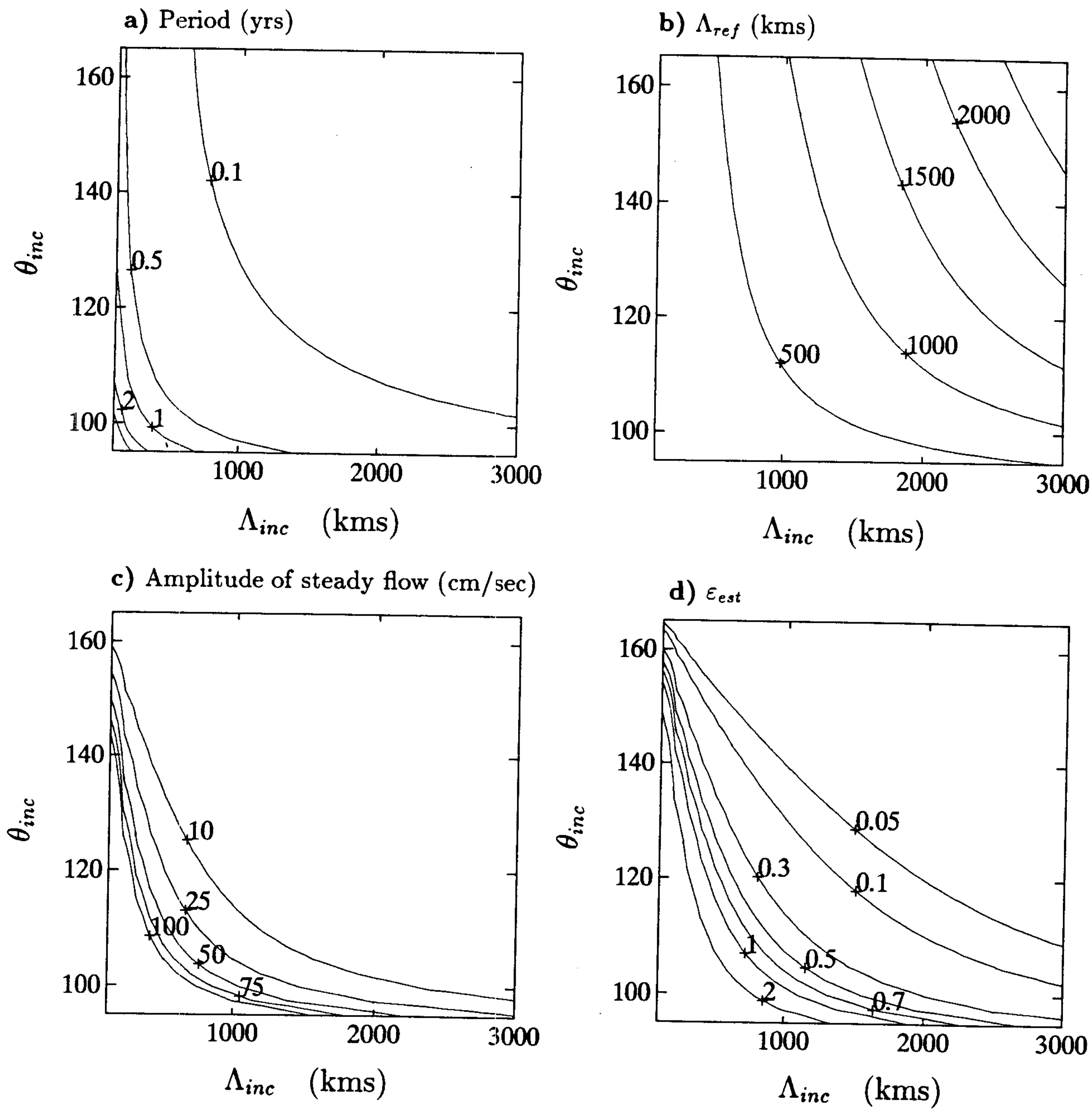

FIG. 6. As in Fig. 5 but for barotropic free surface waves ($n = 0$) and the wave amplitudes calculated from $U_{inc} = 10$ cm s^{-1}. The domain is (100 km, 3000 km) × (95°, 165°).

riodic in y. All maps shown are for *nondimensional* streamfunctions taken at $z = 0$. To get the dimensional streamfunction, one must multiply by $UL = A_*$.

An example of the solution for an annual barotropic free surface RW as the incident wave (parameters of Fig. 1) is shown in Fig. 8. We got $\epsilon_{est} = \epsilon_{true} = 0.79$, $r_{1,0} = 0.90$, $r_{2,0} = 0.68$, and $r_{2,01} = 0.50$; these numbers together with the maps suggest it is a case where nonlinear effects are sufficiently strong to allow their easy recognition, but weak enough to permit a perturbative solution. The solution to first order appears as a substantially distorted $\psi^{(0)}$ (Figs. 8b, d, f). The modifications to $\psi^{(0)}$ and $\psi^{(0)} + \epsilon\psi^{(1)}$ due to the shift in $l_{1,2}$ are very small [Figs. 8a and 8b are almost identical to Figs. 8c and 8d, respectively (the highs and lows in 8c have shortened a bit)]. The first-order correction is the largest and the rms of $\epsilon^2\psi^{(2)}$ relative to the rms of the solution to first order is almost 50%, somewhat more

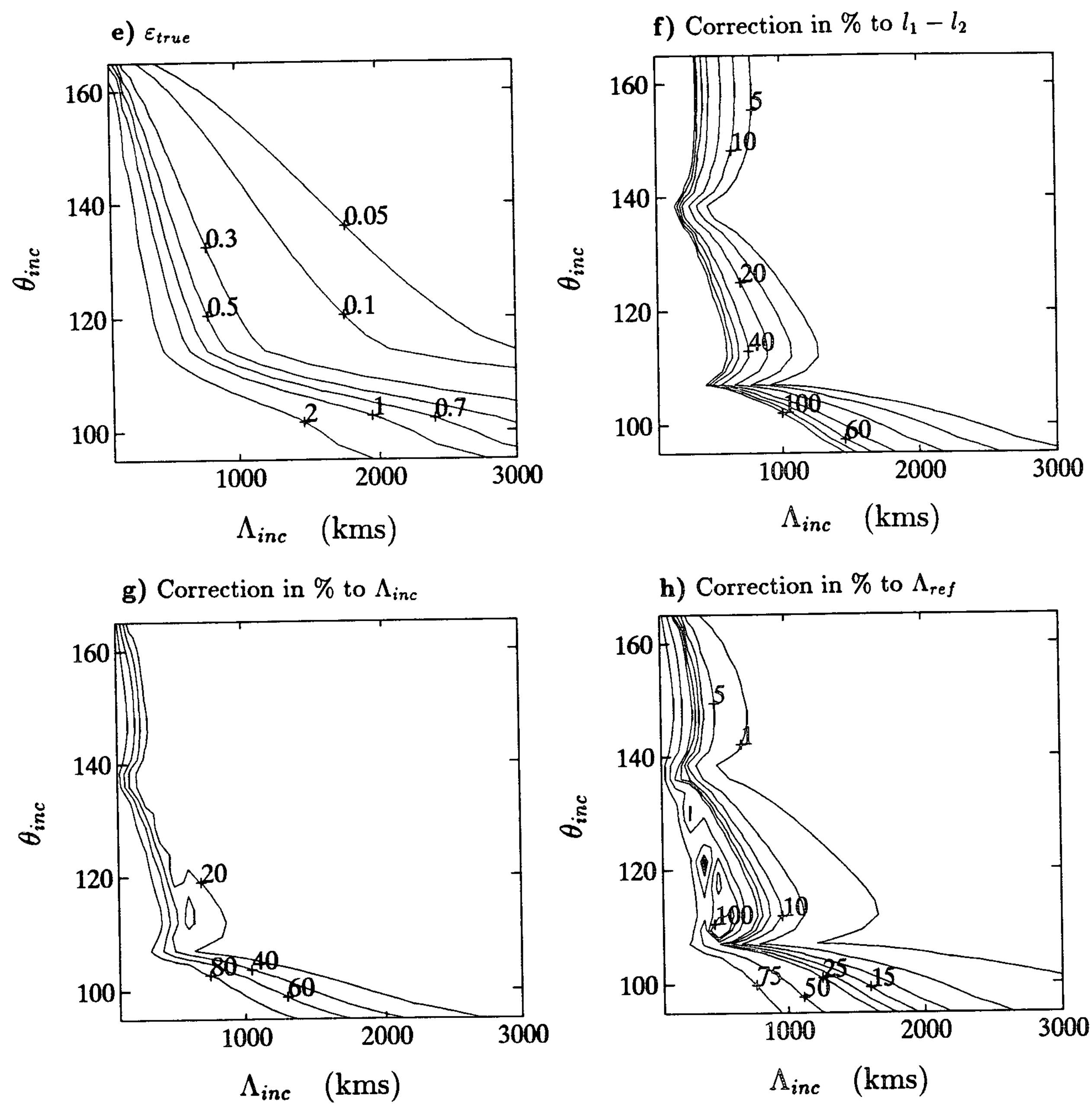

FIG. 6. (*Continued*)

than what one would have guessed by just looking at Figs. 8d–e and 8f–g. Comparing Figs. 8b, 8d, and 8f, one concludes that the correction to η_2 is larger than the correction to $l_1 - l_2$. The consistency of the ratios $r_{i,j}$—for example, $r_{1,0} = 0.91$, 0.92, and 0.90—suggests that although the corrections do change the streamfunctions, they are stable indicators of ratios of rms values.

Another definitely weaker nonlinear case is shown in Fig. 9, where we have chosen a barotropic free surface incident RW with a 36.5-day period. There is little distortion in $\psi^{(0)} + \epsilon\psi^{(1)}$ when compared to $\psi^{(0)}$ (Figs. 9a and 9c). To increase the nonlinearity, we have doubled the wave amplitude in Fig. 10 to $U_{\rm inc} = 10$ cm s^{-1}. Obviously we do not show $\psi^{(0)}$ again [to $O(\epsilon)$], but the solutions up to first order could be compared, and as expected, Fig. 10a looks more distorted than 9c. The correction to the steady flow, that is, to $l_1 - l_2$, is unnoticeable (cf. Figs. 9a with 10b and 10a with 10c), a result that can be confirmed by looking at Fig. 6f at

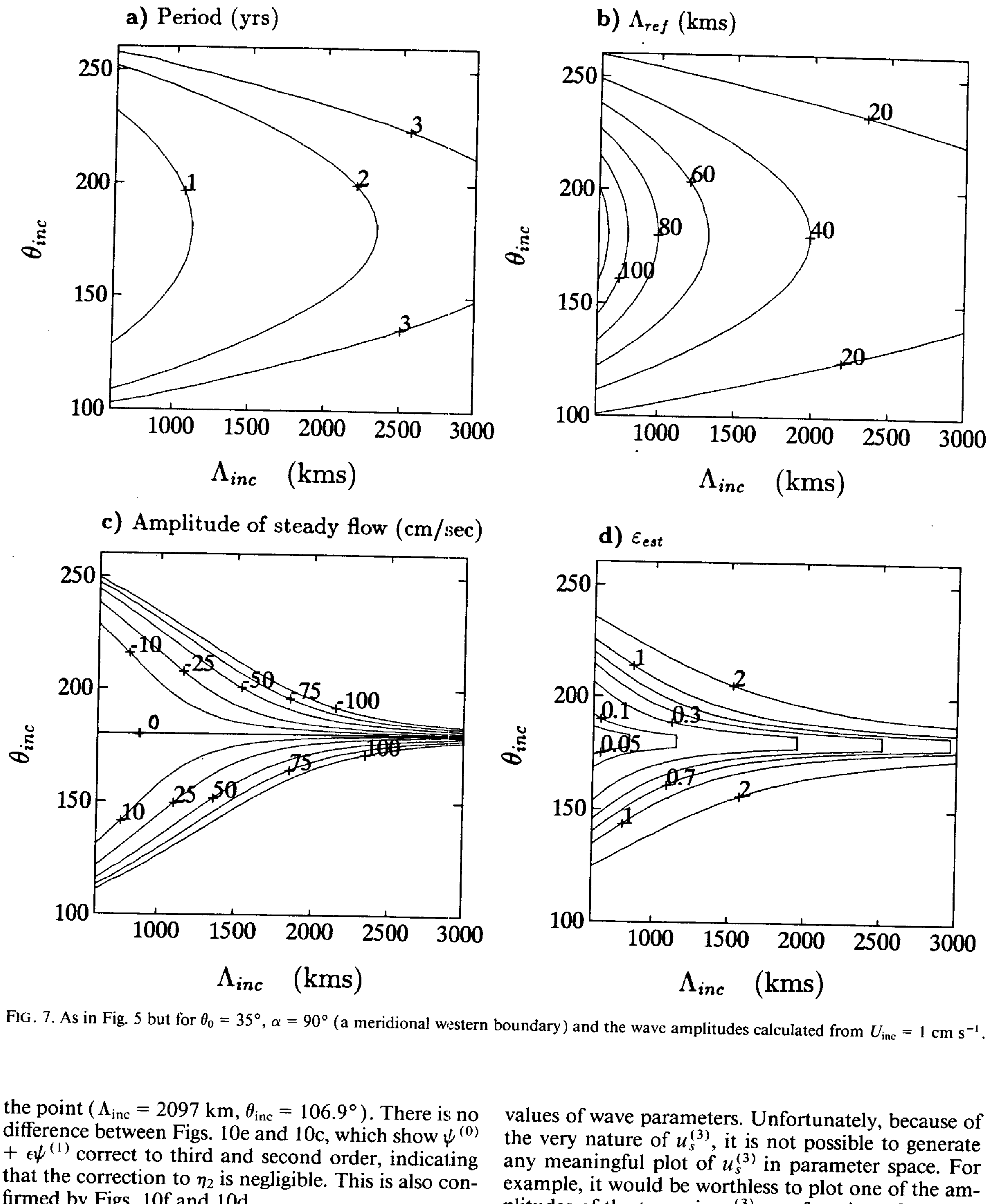

FIG. 7. As in Fig. 5 but for $\theta_0 = 35°$, $\alpha = 90°$ (a meridional western boundary) and the wave amplitudes calculated from $U_{\rm inc} = 1$ cm s^{-1}.

the point ($\Lambda_{\rm inc} = 2097$ km, $\theta_{\rm inc} = 106.9°$). There is no difference between Figs. 10e and 10c, which show $\psi^{(0)} + \epsilon\psi^{(1)}$ correct to third and second order, indicating that the correction to η_2 is negligible. This is also confirmed by Figs. 10f and 10d.

d. Comparing $u_{s*}^{(1)}$ and $u_{s*}^{(1)} + u_{s*}^{(3)}$

We would like to make a comparison between the steady flow at O(ϵ), that is, MM's flow in the absence of friction, and the steady flow up to O(ϵ^3) for different values of wave parameters. Unfortunately, because of the very nature of $u_s^{(3)}$, it is not possible to generate any meaningful plot of $u_s^{(3)}$ in parameter space. For example, it would be worthless to plot one of the amplitudes of the terms in $u_s^{(3)}$ as a function of any two parameters—it would tell us very little about $u_s^{(3)}$. We have to limit the calculation of $u_s^{(3)}$ to just a few cases.

A measure of the magnitude of the O(ϵ^3) correction to the steady flow of MM is given by

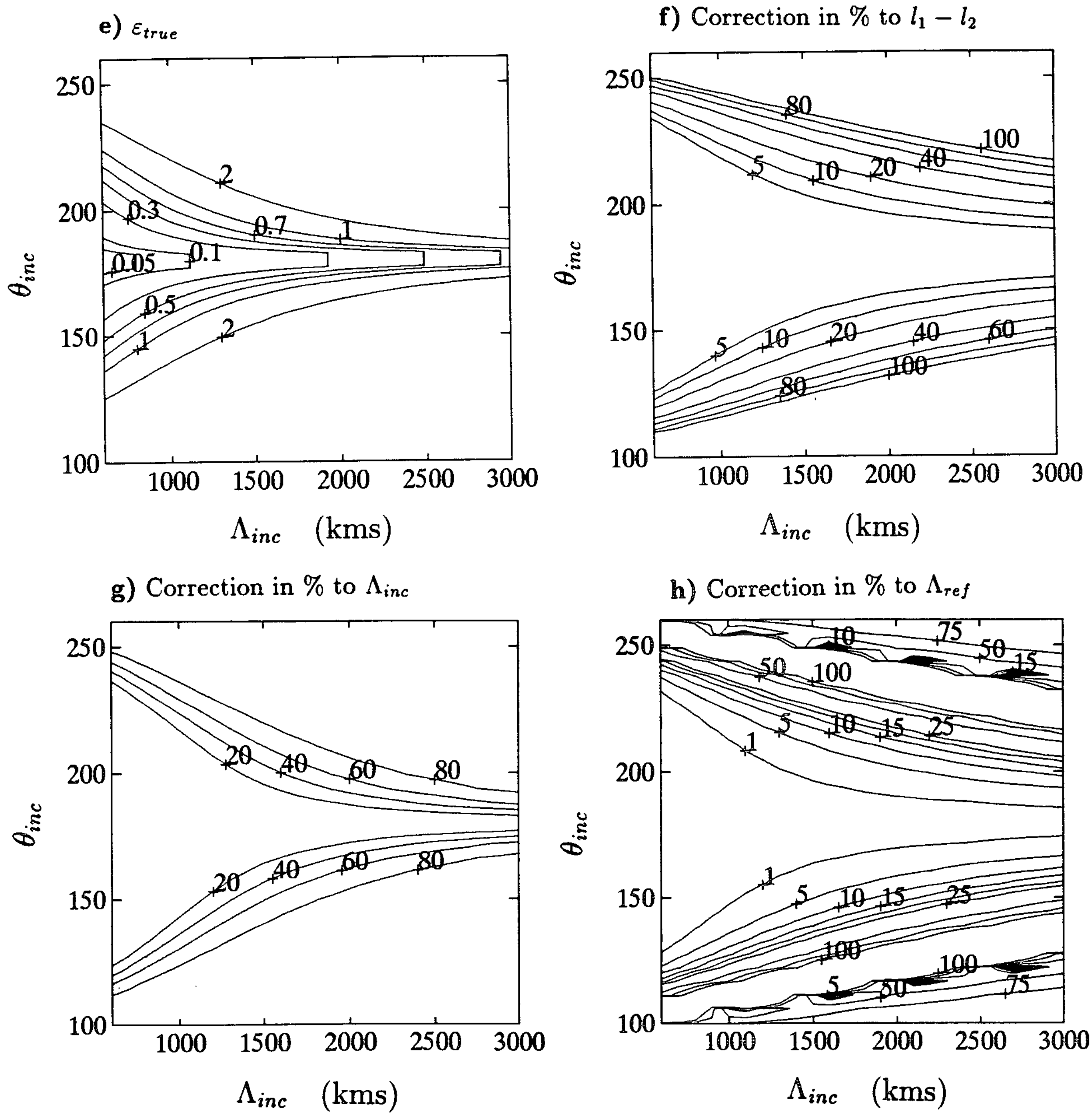

FIG. 7. (*Continued*)

$$r_{u3,1} = \frac{\text{rms}(\epsilon^3 u_s^{(3)})}{\text{rms}(\epsilon u_s^{(1)})} = \epsilon^2 \frac{\sqrt{\sum_y (u_s^{(3)})^2}}{\sqrt{\sum_y (u_s^{(1)})^2}}, \qquad (5.6)$$

where the sum over y must extend at least over one wavelength of $u_s^{(1)}$.

In Figs. 11 and 12 we show two examples (with the parameters of Figs. 1 and 10) of the correction $u_{s*}^{(3)}(y_*)$ and the comparison between $u_{s*}^{(1)}(y_*)$ and $u_{s*}^{(1)}(y_*) + u_{s*}^{(3)}(y_*)$. The first example clearly shows the nonperiodicity of $u_{s*}^{(3)}$. We obtained $r_{u3,1} = 0.40$, which means that the rms of $u_{s*}^{(3)}$ is 40% of the rms of $u_{s*}^{(1)}$. As $r_{u3,1} < r_{2,0} = 0.68$ (Fig. 8) we could say that the second-order correction relative to the zeroth-order solution is more important than the third relative to the first. The ratio $u_{s*}^{(3)}/u_{s*}^{(1)}$ at the coast is 0.64, overestimating $r_{u3,1}$. Note that the largest differences between $u_{s*}^{(1)}$ and $u_{s*}^{(1)} + u_{s*}^{(3)}$ occur near the coast. This example illustrates clearly that for a moderately strong

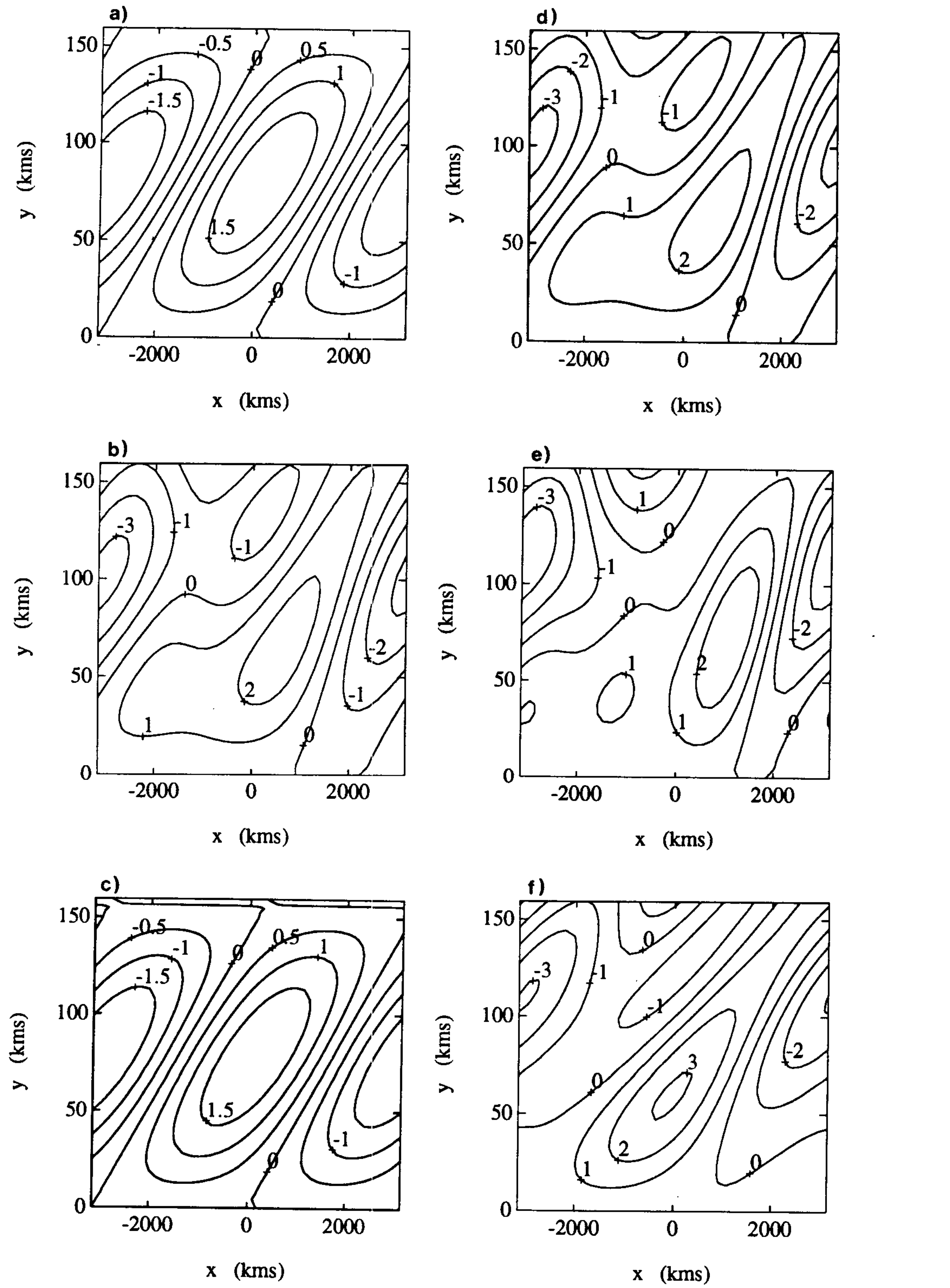

FIG. 8. Instantaneous map of (a) $\psi^{(0)}$; (b) $\psi^{(0)} + \epsilon\psi^{(1)}$, $r_{1,0} = 0.91$; (c) corrected $\psi^{(0)}$, due to shift in $l_{1,2}$; (d) corrected $\psi^{(0)} + \epsilon\psi^{(1)}$, due to shift in $l_{1,2}$, $r_{1,0} = 0.92$; (e) $\psi^{(0)} + \epsilon\psi^{(1)} + \epsilon^2\psi^{(2)}$, correct to $O(\epsilon^2)$, $r_{2,0} = 0.66$, $r_{2,01} = 0.48$; (f) $\psi^{(0)} + \epsilon\psi^{(1)}$, correct to $O(\epsilon^3)$, $r_{1,0} = 0.90$;

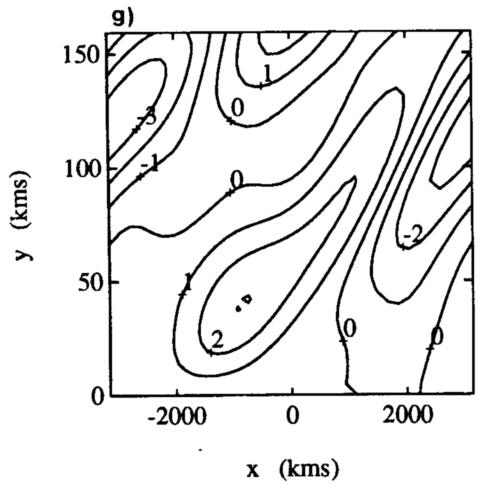

FIG. 8. (*Continued*) and (g) $\psi^{(0)} + \epsilon\psi^{(1)} + \epsilon^2\psi^{(2)}$, correct to $O(\epsilon^3)$, $r_{2,0} = 0.68$, and $r_{2,01} = 0.50$. The parameters are as in Fig. 1.

nonlinear problem with $\epsilon_{est} \sim \epsilon_{true} = 0.79$ and $r_{1,0} = 0.90$

- the $O(\epsilon)$ steady flow is by no means negligible, in this case of the same order of magnitude as U_{ref};
- the transients at $O(\epsilon)$ are very important, of the same order of magnitude of the steady flow;
- the third-order correction is not negligible and substantially changes the MM flow, so that the steady flow up to $O(\epsilon^3)$ is quite different from the $O(\epsilon)$ steady flow.

In the second example (Fig. 12), $u_{s*}^{(3)}$ looks periodic; we got $r_{u3,1} = 0.26$, this time larger than $r_{2,0} = 0.15$ (Fig. 10). As already mentioned, this is a nonlinearly weaker case than the first example. This example has $\epsilon_{est} = 0.12$, $\epsilon_{true} = 0.42$, and $r_{1,0} = 0.30$; it shows that

- the $O(\epsilon)$ steady flow is not negligible, about 45% of U_{inc} and 20% of U_{ref};
- the transients at $O(\epsilon)$ are of the same order of magnitude of the steady flow (not shown in figure);
- the rms of $u_{s*}^{(3)}$ relative to the rms of $u_{s*}^{(1)}$ is 26%.

6. Summary and conclusions

The weak nonlinear interaction of an incident and the reflected RW has been studied. Their interaction at first-order produces

1) a steady forcing that leads to an Eulerian steady mean flow parallel to the nonzonal wall (MM flow without friction); and

2) a transient forcing oscillating in time with a frequency twice that of the incident–reflected RW pair, that is, 2ω.

The steady forcing, whose response is the steady flow, *cannot be resonant,* which implies, under the weak nonlinear regime, that there cannot be energy exchange

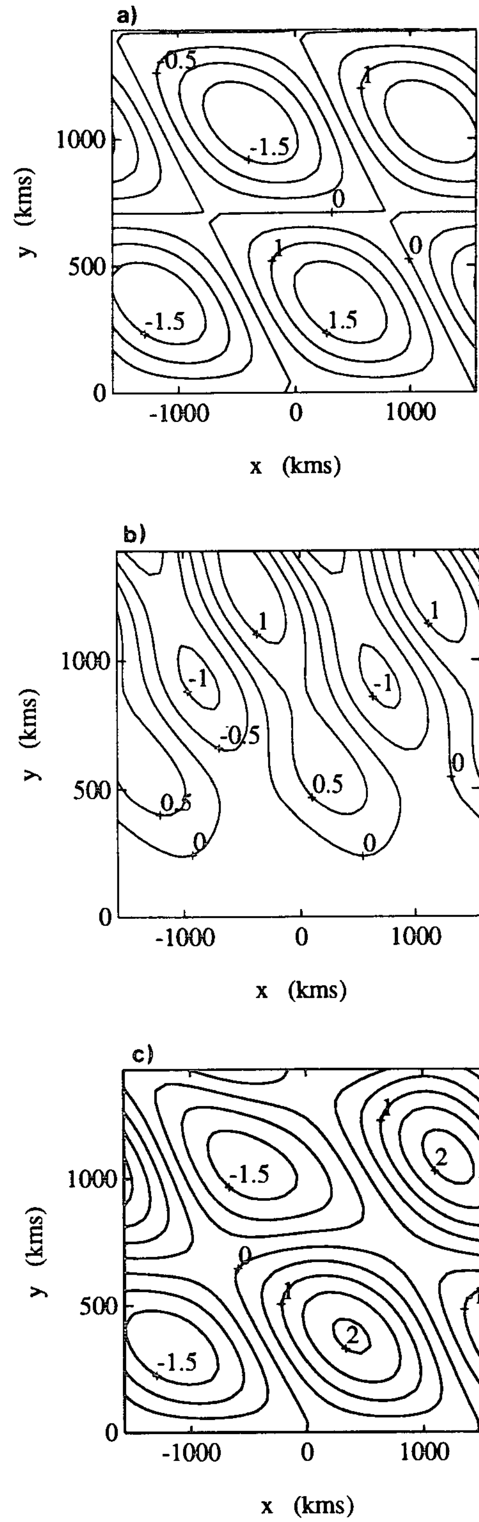

FIG. 9. Instantaneous map of (a) $\psi^{(0)}$; (b) $\psi^{(1)}$; and (c) $\psi^{(0)} + \epsilon\psi^{(1)}$. Parameters: $\theta_0 = 25°$, $\alpha = 25°$, $n = 0$ (free surface), $H = 4500$ m, $T = 0.1$ yr, $k_* = -0.002$ km^{-1}, $\theta_{inc} = 106.9°$, $U_{inc} = 5$ cm s^{-1}, $U_{ref} = 11.6$ cm s^{-1}, $\Lambda_{inc} = 2097$ km, $\Lambda_{ref} = 907$ km, $\phi_{inc} = 213.5°$, $\epsilon = \max(\epsilon_{inc}, \epsilon_{ref}) = 0.27$, $\epsilon_{est} = 0.06$, $\epsilon_{true} = 0.21$, and $r_{1,0} = 0.16$.

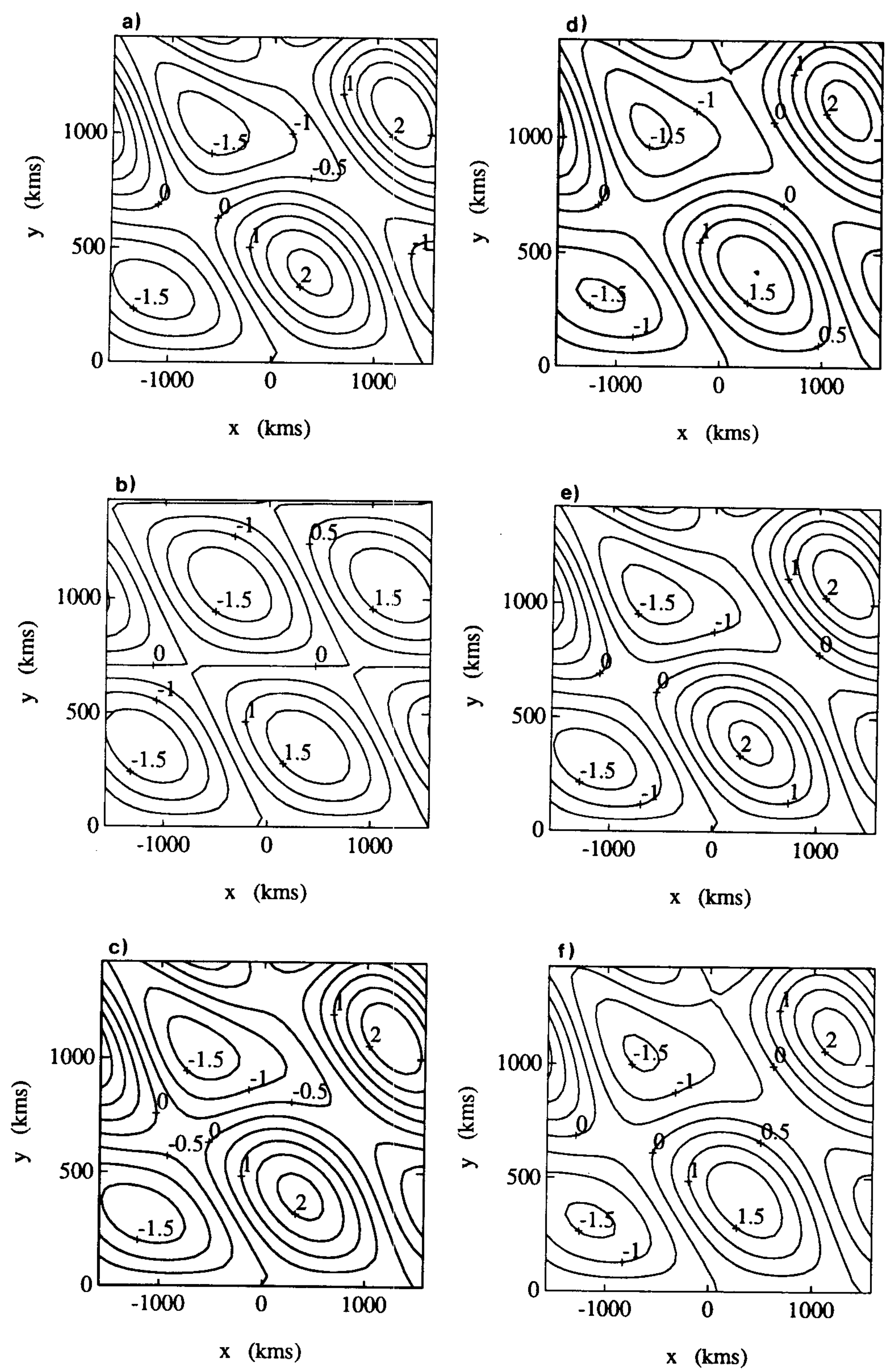

FIG. 10. Instantaneous map of (a) $\psi^{(0)} + \epsilon\psi^{(1)}$, $r_{1,0} = 0.32$; (b) corrected $\psi^{(0)}$, due to shift in $l_{1,2}$; (c) corrected $\psi^{(0)} + \epsilon\psi^{(1)}$, due to shift in $l_{1,2}$, $r_{1,0} = 0.32$; (d) $\psi^{(0)} + \epsilon\psi^{(1)} + \epsilon^2\psi^{(2)}$, correct to $O(\epsilon^2)$, $r_{2,0} = 0.15$, $r_{2,01} = 0.15$; (e) $\psi^{(0)} + \epsilon\psi^{(1)}$, correct to $O(\epsilon^3)$, $r_{1,0} = 0.30$, and (f) $\psi^{(0)} + \epsilon\psi^{(1)} + \epsilon^2\psi^{(2)}$, correct to $O(\epsilon^3)$, $r_{2,0} = 0.15$, and $r_{2,0:} = 0.14$. The parameters are as in Fig. 9 but with a larger wave amplitude: $U_{inc} = 10$ cm s^{-1}, $U_{ref} = 23.1$ cm s^{-1}, $\epsilon = \max(\epsilon_{inc}, \epsilon_{ref}) = 0.53$, $\epsilon_{est} = 0.12$, and $\epsilon_{true} = 0.42$.

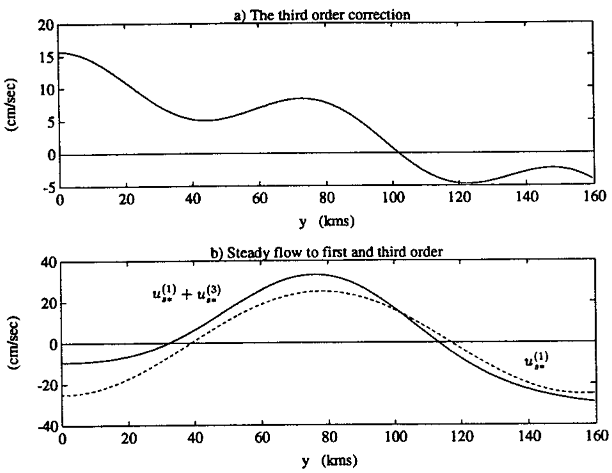

FIG. 11. (a) The O(ϵ^3) correction (in cm s^{-1}) to the steady flow—that is, $u_{s*}^{(3)}$—vs distance from the wall. (b) A comparison between the steady flow at O(ϵ), $u_{s*}^{(1)}$ (dashed line), and the steady flow up to O(ϵ^3), $u_{s*}^{(1)} + u_{s*}^{(3)}$ (solid line), as a function of distance from the wall. The parameters are as in Fig. 1; $r_{u3,1} = 0.40$.

between the steady flow and the incoming and reflected RW; the steady flow is neutrally *stable* to the RWs that generated it in the first place. This is true for any number of incident–reflected RW pairs, but does not imply that the RW-driven steady flow is stable; it could very well be unstable to other perturbations.

The response to the transient or 2ω forcing consists of two parts: a direct (forced solution) and an indirect response (homogeneous solution, needed to balance out the forced flow normal to the wall). The transient forcing can be resonant, but only if $0 < |\sin\alpha| \leq 1/3$, that is, for more zonally oriented walls (Graef 1993).

At second order, the nonlinear interaction between the incident–reflected RW field and the forced first-order flow (steady plus transient) produces, in general, resonant forcing, which leads to a modification of the RWs' phases: a shift in their offshore wavenumber. Therefore, the effect of the steady flow plus 2ω transients on the incident–reflected RW pair is to change their offshore wavenumber.

The O(ϵ^2) correction to $\psi^{(0)}$ influences $\psi^{(1)}$ through the steady flow $u_s^{(1)}$; qualitatively, the widths of the steady currents in MM flow are modified.

In contrast to first-order nonlinear interactions, where one has to search for resonant triads, there is always resonant forcing at O(ϵ^2), unless the coupling coefficient vanishes (in general it will not). Resonant forcing is thus the rule rather than the exception.

The analytical solution allows us to compute some of the corrections to $l_{1,2}$, etc., as a function of (Λ_{inc}, θ_{inc}), that is, to explore some characteristics of the solution in parameter space.

There is no steady forcing at all at O(ϵ^2); hence it becomes necessary to go one order higher to see the next correction to MM steady flow.

The steady flow occurring at O(ϵ^3), $u_s^{(3)}$ is driven by the modified RWs as well as through interactions of several components of the solution up to second order. Two examples of $u_s^{(3)}$ were shown: one in which the rms of the third-order correction $u_{s*}^{(3)}$ was 40% of the rms of $u_{s*}^{(1)}$, which is perhaps too strongly nonlinear,[3] and the other, clearly a (nonlinearly) weaker case, in which $r_{u3,1} = 26\%$. There are cases for which the third-order correction to $u_s^{(1)}$ can be negligible, or of the order of $u_s^{(1)}$, or unrealistically large.

An analysis of the second-order resonances and of the amplitudes of the terms in $u_s^{(3)}$ leads to the following remarkable result: if $|\sin\alpha| > 1/3$ then $u_s^{(3)}$ is bounded. In other words, the entire steady circulation induced by the nonlinear dynamics, up to third order in ϵ, *is immune* to resonances for $|\sin\alpha| > 1/3$, except for those resonances that lead to a shift in the offshore wavenumbers of the RWs.

A fair comparison between the theoretically predicted mean current and observations requires data that allow averaging along the coast or in time to eliminate the transients and the incident–reflected RW pair. The 2ω transient flow at O(ϵ) is of the same order of magnitude of the steady flow $u_s^{(1)}$.

Recent observations relevant to this paper have been made in the Hawaii Ocean Time-Series (HOT) project (Chiswell and Lukas 1990; Chiswell et al. 1990; Winn et al. 1992; Winn et al. 1993). Preliminary results from current measurements (E. Firing 1993, personal communication) on the northeastern side of the Hawaiian Ridge along a section perpendicular to it and averaged over a period from October 1988 through January 1993 show significant resemblance to the North Hawaiian Ridge Current predicted by MM. These observational

[3] For this case, the condition for weak nonlinearity would be only marginally satisfied.

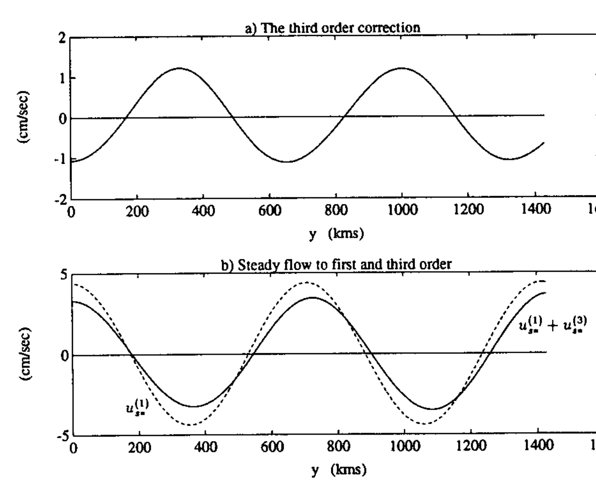

FIG. 12. As in Fig. 11 but with the parameters of Fig. 10; $r_{u3,1} = 0.26$.

results emphasize the importance and potential applicability of our work.

It is clear (e.g., see Figs. 6, 7, and 8) that the reflection problem of RWs can be strongly nonlinear. In many cases, and using more or less realistic wave parameters, the β-Rossby number, chosen to be the maximum between that of the incident and reflected RW, is larger than one. Although this does not necessarily imply that the reflection problem is highly nonlinear and that our perturbation expansion is invalid, it may give an indication of the strength of the nonlinear terms. We believe that to actually validate the expansion, one must calculate the $r_{i,j}$, but this implies, of course, computing the solution.

By a systematic use of perturbation expansion and multiple scales, the following picture emerges:

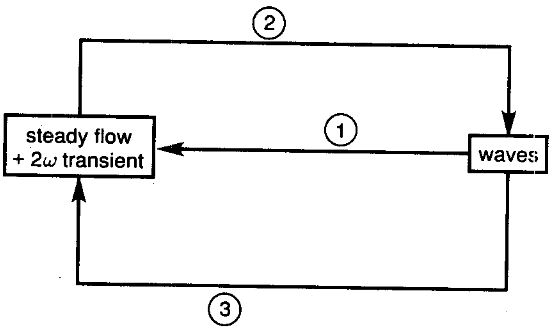

There is a clear feedback between the waves and the steady flow: in a very simplistic way, the waves produce the steady current, the current affects the waves, which change the current, . . . and so on.

Future work

This (hopefully) improved theory of the steady current driven by the nonlinear interaction of an incoming and the reflected RW has a flat bottom. For example, the topography of the real Hawaiian Ridge is complex and can probably not be considered in analytical calculations. Also, the stability of the steady flow would have to be addressed (perhaps). One disregards the origin of such flow[4] and studies its stability. The nonzonal steady flow is an exact nonlinear solution to a *forced* QGPVE. However, when the steady flow plus the perturbation is plugged into the forced QGPVE, the forcing drops out. One is left with a PDE having coefficients that are periodic functions of y and z. Nonzonal flows are in general more unstable than pure zonal flows (Pedlosky 1979).

The theory developed here assumes an inviscid fluid. Dissipation effects are expected to play an important role near solid boundaries and there is no doubt that adding friction to the model will make it more realistic. On the other hand, it will make the algebra even more cumbersome. For western boundaries, the reflected RWs are short and thus more susceptible to dissipation. Mysak and Magaard incorporated Rayleigh friction (acting only on the short reflected wave) in their model; as a consequence, the steady flow had an exponentially decaying (in y) amplitude and became a true boundary current.

Finally, it is encouraging that recent observations have provided the first significant evidence supporting the existence of the North Hawaiian Ridge Current. However, an actual application (e.g., a full comparison between our theory and observations) would lie outside the scope of this paper. Furthermore, the interannual fluctuations of the observed currents poses additional challenging questions: Theoretically, the secondary flow is steady, but there exists the possibility of having resonant interactions between three incident–reflected RW pairs, which would imply that the amplitudes of the flows parallel to the wall would fluctuate slowly in time (Graef 1993). In view of the observed fluctuations, it may be worth exploring this possibility further.

Acknowledgments. The authors want to thank Peter Muller for helpful discussions and his interest in this work. We are particularly grateful to Eric Firing who has most generously provided us with unpublished results of current measurements from the HOT cruises. Antoine Badán, Pedro Ripa, and Julio Sheinbaum made valuable comments and suggestions on the manuscript. Part of this work is the first author's dissertation at the University of Hawaii; the paper was completed at CICESE and funded by the SPP and SEP of Mexico and by CONACYT under Grant 1002-T9111.

APPENDIX

Forcing for $\psi^{(3)}$

Since $\psi^{(1)}$ (because of $\psi^{(1)}_{\rm hom}$) and $\psi^{(2)}$ depend on where k lies, the forcing for $\psi^{(3)}$ will also depend on k and we would have two cases as in section 3c. However, we saw at the end of section 3c that case 2 reduces to case 1 if we put $\eta^{(i)} = 0$, $\eta^{(r)} = \eta_2$, and $\theta_r^{(1)} = \theta_2^{(1)}$; thus, we will consider only the second case.

There is an additional consideration when η is real (case 1). The forcing for $\psi^{(3)}$ contains terms $\sim \cos\theta_2^{(1)}$—that is, homogeneous solutions of (4.1)—that would produce secular terms unless they are eliminated. This is accomplished if we write the phase of $\psi^{(1)}_{\rm hom}$ as

$$\theta_2^{(1)} = 2kx + \eta_2 y - 2\omega t + 2\phi + \phi^{(1)}(Y_2, \cdots), \tag{A.1}$$

with $\phi^{(1)}(0, \cdots) = 0$ to satisfy the BC at the wall (2.5). The introduction of $\phi^{(1)}$ is analogous to what

[4] Whether this is conceptually correct is not a trivial question. Keep in mind that the very existence of the steady current is due to the nonlinear interaction of incoming and outgoing RWs.

we did at second order with $\psi^{(0)}$ using multiple scales; now it is done with $\psi^{(1)}_{\rm hom}$ at third order. Note, though, that here it is only in the phase of $\psi^{(1)}_{\rm hom}$ that we have the freedom of adding a dependence on Y_2, since its amplitude, $\sim B_{12}$, is fixed and turned out to be independent of Y_2. As usual, the dependence of $\phi^{(1)}$ on Y_2 is found when secular terms are eliminated (shown below). In case 2, although there are several forcing terms on the rhs of (4.1) that are homogeneous solutions of it, specifically those

$$\sim e^{-\eta^{(i)}y} \begin{matrix}\sin\\ \cos\end{matrix} \theta_r^{(1)},$$

these forcing terms do *not* produce secular terms. The response (or particular solution) to such forcing functions is *bounded:*

$$\sim ye^{-\eta^{(i)}y} \begin{matrix}\cos\\ \sin\end{matrix} \theta_r^{(1)}.$$

These are clearly uniformly valid solutions in y and there is no need in this case to introduce a phase $\phi^{(1)}(Y_2, \cdots)$ in $\psi^{(1)}_{\rm hom}$.

The three Jacobians on the rhs of (4.1) give

$$\begin{aligned}
&J(\psi^{(0)}, \nabla^2\psi^{(2)}) + J(\psi^{(1)}, \nabla^2\psi^{(1)}) + J(\psi^{(2)}, \nabla^2\psi^{(0)})\\
&= \frac{1}{2}Ak \sum_{i=1}^{2}\sum_{j=1}^{2} [C_{2+i,j}[\cos(\theta_j^{(0)} - 2\theta_i^{(0)} + \delta_{i2}\theta_1^{(0)} + \delta_{i1}\theta_2^{(0)}) - \cos(\theta_j^{(0)} + 2\theta_i^{(0)} - \delta_{i2}\theta_1^{(0)} - \delta_{i1}\theta_2^{(0)})]\\
&\quad + e^{-\eta^{(i)}y}\{C_{4+i,s,j}[\cos(\theta_j^{(0)} - \theta_i^{(0)} - \theta_r^{(1)}) - \cos(\theta_j^{(0)} + \theta_i^{(0)} + \theta_r^{(1)})] + S_{4+i,s,j}[\sin(\theta_j^{(0)} - \theta_i^{(0)} - \theta_r^{(1)})\\
&\quad + \sin(\theta_j^{(0)} + \theta_i^{(0)} + \theta_r^{(1)})] + C_{4+i,d,j}[\cos(\theta_j^{(0)} - \theta_i^{(0)} + \theta_r^{(1)}) - \cos(\theta_j^{(0)} + \theta_i^{(0)} - \theta_r^{(1)})]\\
&\quad + S_{4+i,d,j}[\sin(\theta_j^{(0)} - \theta_i^{(0)} + \theta_r^{(1)}) + \sin(\theta_j^{(0)} + \theta_i^{(0)} - \theta_r^{(1)})]\} + C_{6+i,j}[\cos(\theta_j^{(0)} - 2\theta_i^{(0)} - \delta_{i2}\theta_1^{(0)} - \delta_{i1}\theta_2^{(0)})\\
&\quad - \cos(\theta_j^{(0)} + 2\theta_i^{(0)} + \delta_{i2}\theta_1^{(0)} + \delta_{i1}\theta_2^{(0)})] + H_{ij}[\cos(\theta_j^{(0)} - \theta_2^{(0)}) - \cos(\theta_j^{(0)} + \theta_2^{(0)})]\\
&\quad + H_{4+i,d,j}[\sin(\theta_j^{(0)} - \theta_2^{(0)}) + \sin(\theta_j^{(0)} + \theta_2^{(0)})] + e^{-\mu^{(i)}y}\{P_{ij}[\sin(\theta_j^{(0)} + \theta_r^{(2)}) + \sin(\theta_j^{(0)} - \theta_r^{(2)})]\\
&\quad + Q_{ij}[\cos(\theta_j^{(0)} - \theta_r^{(2)}) - \cos(\theta_j^{(0)} + \theta_r^{(2)})]\}] + G_6 e^{-2\eta^{(i)}y}\\
&\quad + \frac{B_{12}^2 k}{2\omega\lambda'}\sum_{i=1}^{2}[G_1\cos 2\theta_i^{(0)} + e^{-\eta^{(i)}y}\{G_2\cos[\theta_r^{(1)} + (-1)^i(\theta_2^{(0)} - \theta_1^{(0)})] + G_3\cos[\theta_1^{(0)} + \theta_2^{(0)} + (-1)^i\theta_r^{(1)}]\\
&\qquad + G_4\sin[\theta_r^{(1)} + (-1)^i(\theta_1^{(0)} + \theta_2^{(0)})] + G_5\sin[\theta_r^{(1)} + (-1)^i(\theta_2^{(0)} - \theta_1^{(0)})]\}], \quad (A.2)
\end{aligned}$$

where the coefficients in (A.2) are, for $i, j = 1, 2$:

$$C_{2+i,j} = (-1)^j A_{2+i}^{(2)}[(2l_i - \delta_{i1}l_2 - \delta_{i2}l_1)^2 - l_j^2](2l_i - \delta_{i1}l_2 - \delta_{i2}l_1 - l_j) \quad (A.3)$$

$$C_{4+i,s,j} = (-1)^j\{(-\eta^{(i)})PR_i + PM_i(3l_j - l_i - \eta^{(r)}) + (k^2 + l_j^2)[A_{8+i,s}^{(2)}(3l_j - l_i - \eta^{(r)}) - \eta^{(i)}A_{4+i,s}^{(2)}]\} \quad (A.4)$$

$$S_{4+i,s,j} = (-1)^j\{(-\eta^{(i)})PM_i + PR_i(l_i + \eta^{(r)} - 3l_j) + (k^2 + l_j^2)[A_{4+i,s}^{(2)}(l_i + \eta^{(r)} - 3l_j) - \eta^{(i)}A_{8+i,s}^{(2)}]\} \quad (A.5)$$

$$C_{4+i,d,j} = (-1)^j\{(-\eta^{(i)})PN_i - PV_i(l_i - \eta^{(r)} + l_j) + (k^2 + l_j^2)[A_{8+i,d}^{(2)}(\eta^{(r)} - l_i - l_j) - \eta^{(i)}A_{4+i,d}^{(2)}]\} \quad (A.6)$$

$$S_{4+i,d,j} = (-1)^j\{(-\eta^{(i)})PV_i + PN_i(l_i - \eta^{(r)} + l_j) + (k^2 + l_j^2)[A_{4+i,d}^{(2)}(l_i - \eta^{(r)} + l_j) - \eta^{(i)}A_{8+i,d}^{(2)}]\} \quad (A.7)$$

$$C_{6+i,j} = (-1)^j A_{6+i}^{(2)}[(3k)^2 + (2l_i + \delta_{i2}l_1 + \delta_{i1}l_2)^2 - k^2 - l_j^2](2l_i + \delta_{i2}l_1 + \delta_{i1}l_2 - 3l_j) \quad (A.8)$$

$$H_{ij} = (-1)^j(A_{2+i}^{(2)} + A_{8+i,d}^{(2)})(l_j^2 - l_2^2)(l_2 - l_j) \quad (A.9)$$

$$H_{4+i,d,j} = (-1)^j A_{4+i,d}^{(2)}(l_j^2 - l_2^2)(l_2 - l_j) \quad (A.10)$$

$$P_{ij} = (-1)^j\{PA_i(\mu^{(r)} - 3l_j) + PG_i(-\mu^{(i)}) + (k^2 + l_j^2)[(A_{8+i,s}^{(2)} + A_{6+i}^{(2)})\mu^{(i)} + A_{4+i,s}^{(2)}(3l_j - \mu^{(r)})]\} \quad (A.11)$$

$$Q_{ij} = (-1)^j\{PG_i(3l_j - \mu^{(r)}) + PA_i(-\mu^{(i)}) + (k^2 + l_j^2)[(A_{8+i,s}^{(2)} + A_{6+i}^{(2)})(\mu^{(r)} - 3l_j) + \mu^{(i)}A_{4+i,s}^{(2)}]\}, \quad (A.12)$$

where in turn

$$\left.\begin{aligned}
PR_i &= A^{(2)}_{4+i,s}[-(3k)^2 - (l_i + \eta^{(r)})^2 + \eta^{(i)^2}] + 2\eta^{(i)}A^{(2)}_{8+i,s}(l_i + \eta^{(r)})\\
PM_i &= A^{(2)}_{8+i,s}[-(3k)^2 - (l_i + \eta^{(r)})^2 + \eta^{(i)^2}] - 2\eta^{(i)}A^{(2)}_{4+i,s}(l_i + \eta^{(r)})\\
PN_i &= A^{(2)}_{4+i,d}[-k^2 - (l_i - \eta^{(r)})^2 + \eta^{(i)^2}] + 2\eta^{(i)}A^{(2)}_{8+i,d}(l_i - \eta^{(r)})\\
PV_i &= A^{(2)}_{8+i,d}[-k^2 - (l_i - \eta^{(r)})^2 + \eta^{(i)^2}] - 2\eta^{(i)}A^{(2)}_{4+i,d}(l_i - \eta^{(r)})\\
PA_i &= A^{(2)}_{4+i,s}[(3k)^2 + \mu^{(r)^2} - \mu^{(i)^2}] - (A^{(2)}_{8+i,s} + A^{(2)}_{6+i})2\mu^{(i)}\mu^{(r)}\\
PG_i &= A^{(2)}_{4+i,s}2\mu^{(i)}\mu^{(r)} + (A^{(2)}_{8+i,s} + A^{(2)}_{6+i})[(3k)^2 + \mu^{(r)^2} - \mu^{(i)^2}]
\end{aligned}\right\}. \tag{A.13}$$

The remaining coefficients are

$$\left.\begin{aligned}
G_1 &= \frac{(2k)^2 + (l_1 + l_2)^2 - (l_1 - l_2)^2}{\sin\alpha}\\
G_2 &= \frac{(l_1 - l_2)^2 - (2k)^2 - \eta^{(r)^2} + \eta^{(i)^2}}{\sin\alpha}\\
G_3 &= \frac{[\eta^{(r)^2} - \eta^{(i)^2} - (l_1 + l_2)^2][\eta^{(r)} - (l_1 + l_2)] - 2\eta^{(i)^2}\eta^{(r)}}{2\omega\lambda'}\\
G_4 &= \frac{\eta^{(i)}}{2\omega\lambda'}[(l_1 + l_2)^2 - 3\eta^{(r)^2} + \eta^{(i)^2} + 2(l_1 + l_2)\eta^{(r)}]\\
G_5 &= \frac{2\eta^{(i)}\eta^{(r)}}{\sin\alpha}\\
G_6 &= \left(\frac{B_{12}}{2\omega\lambda'}\right)^2 4k\eta^{(i)^2}\eta^{(r)}
\end{aligned}\right\}. \tag{A.14}$$

The fourth and fifth terms on the rhs of (4.1) are $-J_{xY_2}(\psi^{(0)}, \nabla^2\psi^{(0)})$, where J_{xY_2} is the Jacobian operator with respect to x and Y_2. Analogously, the sixth and seventh terms are $-2J(\psi^{(0)}, \partial_{yY_2}\psi^{(0)})$.We obtain

$$J_{xY_2}(\psi^{(0)}, \nabla^2\psi^{(0)}) + 2J(\psi^{(0)}, \partial_{yY_2}\psi^{(0)}) = B^{(2)}_{12}[\cos(\theta_1^{(0)} - \theta_2^{(0)}) - \cos(\theta_1^{(0)} + \theta_2^{(0)})], \tag{A.15}$$

where $B^{(2)}_{12} = \frac{1}{2}A^2k(l_2 - l_1)[3(l_2^{(2)}l_2 - l_1^{(2)}l_1) + l_1l_2^{(2)} - l_2l_1^{(2)}]$. The higher-order contribution to the steady flow on the rhs of (A.15) arise from the $O(\epsilon^2)$ correction to $\psi^{(0)}$. As in first order, the nonlinear interaction of the now modified incident and reflected RW produces a steady flow parallel to the wall. The next forcing terms are, upon recalling that $A = A(Y_3, \cdots)$ and $\phi = \phi(Y_3, \cdots)$ (see section 3b),

$$\begin{aligned}
2\partial_t\partial_{yY_3}\psi^{(0)} + \sin\alpha\partial_{Y_3}\psi^{(0)} &= (2\omega l_1 + \sin\alpha)(\partial_{Y_3}A\cos\theta_1^{(0)} - A\partial_{Y_3}\phi\sin\theta_1^{(0)})\\
&\quad - (2\omega l_2 + \sin\alpha)(\partial_{Y_3}A\cos\theta_2^{(0)} - A\partial_{Y_3}\phi\sin\theta_2^{(0)}).
\end{aligned} \tag{A.16}$$

Finally, if η is real,

$$\begin{aligned}
2\partial_t\partial_{yY_2}\psi^{(1)} + \sin\alpha\partial_{Y_2}\psi^{(1)} &= (4\omega\eta_2 + \sin\alpha)\frac{B_{12}}{2\omega\lambda'}\partial_{Y_2}\phi^{(1)}\cos\theta_2^{(1)}\\
&\quad - \frac{B_{12}}{(l_1 - l_2)}\partial_{Y_2}(\phi_1 - \phi_2)\cos(\theta_1^{(0)} - \theta_2^{(0)}),
\end{aligned} \tag{A.17}$$

where we have used that $\partial_{Y_2}(\theta_1^{(0)} + \theta_2^{(0)}) = 0$ and $\partial_{Y_2}B_{12} = 0$, since $B_{12} \sim A^2$ is not a function of Y_2; or, if η is complex, $\partial_{Y_2}\psi^{(1)}_{\text{hom}} = 0$, so that

$$\begin{aligned}
2\partial_t\partial_{yY_2}\psi^{(1)} + \sin\alpha\partial_{Y_2}\psi^{(1)} &= \frac{-B_{12}}{(l_1 - l_2)}\partial_{Y_2}(\phi_1 - \phi_2)\cos(\theta_1^{(0)} - \theta_2^{(0)})\\
&= \frac{-kB_{12}^2C_0}{\omega(l_1 - l_2)^2}\cos(\theta_1^{(0)} - \theta_2^{(0)}).
\end{aligned} \tag{A.18}$$

The complete forcing for $\psi^{(3)}$ is given by the sum of (A.2), (A.15), (A.16), and (A.17) or (A.18). The forcing that would produce secular terms in $\psi^{(3)}$ is eliminated by demanding that

$$\partial_{Y_3}A = \partial_{Y_3}\phi = 0, \tag{A.19}$$

and in case η is real

$$(4\omega\eta_2 + \sin\alpha)\frac{B_{12}}{2\omega\lambda'}\partial_{Y_2}\phi^{(1)} + \frac{1}{2}Ak(C_{5,s,1} + C_{6,s,2} + C_{5,d,1} + C_{6,d,2}) = 0, \quad \text{(A.20)}$$

which immediately implies that $A = A(Y_4, \cdots)$, $\phi = \phi(Y_4, \cdots)$, and $\phi^{(1)} \sim Y_2$. As far as their dependence on Y_3 is concerned, A and ϕ can be considered constants. That $\phi^{(1)}$ depends linearly on Y_2 we can interpret as an $O(\epsilon^2)$ correction to the offshore wavenumber η_2; that is, we now see a modification (two orders higher) in the RW $\psi^{(1)}_{\text{hom}}$.

For completeness, we write down the governing equation for $\psi^{(3)}$:

$$\begin{aligned}
\mathcal{M}_0[\psi^{(3)}] = {} & \left[-\frac{1}{2}Ak(C_{31}+C_{42}+H_{11}+H_{21}) - B_{12}^{(2)} + \frac{kB_{12}^2C_0}{\omega(l_1-l_2)^2}\right]\cos(\theta_1^{(0)}-\theta_2^{(0)}) \\
& -\frac{1}{2}Ak[(H_{5,d,1}+H_{6,d,1})\sin(\theta_1^{(0)}-\theta_2^{(0)}) + (C_{32}+C_{41})\cos 2(\theta_1^{(0)}-\theta_2^{(0)})] \\
& + e^{-\eta^{(i)}y}\Bigg\{\left[\frac{1}{2}Ak(C_{5,d,2}+C_{6,d,1}) - \frac{B_{12}^2k}{2\omega\lambda'}G_3\right]\cos(\theta_1^{(0)}+\theta_2^{(0)}-\theta_r^{(1)}) \\
& - \left[\frac{1}{2}Ak(S_{5,d,2}+S_{6,d,1}) - \frac{B_{12}^2k}{2\omega\lambda'}G_4\right]\sin(\theta_1^{(0)}+\theta_2^{(0)}-\theta_r^{(1)}) + \frac{1}{2}Ak[C_{5,d,1}\cos(2\theta_1^{(0)}-\theta_r^{(1)}) \\
& + C_{6,d,2}\cos(2\theta_2^{(0)}-\theta_r^{(1)}) - S_{5,d,1}\sin(2\theta_1^{(0)}-\theta_r^{(1)}) - S_{6,d,2}\sin(2\theta_2^{(0)}-\theta_r^{(1)})]\Bigg\} - G_6e^{-2\eta^{(i)}y} \\
& - \left[\frac{1}{2}Ak(C_{71}+C_{82}-H_{11}-H_{21}) - B_{12}^{(2)}\right]\cos(\theta_1^{(0)}+\theta_2^{(0)}) - \frac{1}{2}Ak(H_{5,d,1}+H_{6,d,1})\sin(\theta_1^{(0)}+\theta_2^{(0)}) \\
& + \left[\frac{1}{2}Ak(C_{32}-C_{72}) - \frac{B_{12}^2k}{2\omega\lambda'}G_1\right]\cos 2\theta_1^{(0)} + \left[\frac{1}{2}Ak(C_{41}-C_{81}) - \frac{B_{12}^2k}{2\omega\lambda'}G_1\right]\cos 2\theta_2^{(0)} \\
& + \frac{1}{2}Ak[C_{31}\cos(3\theta_1^{(0)}-\theta_2^{(0)}) + C_{42}\cos(3\theta_2^{(0)}-\theta_1^{(0)})] \\
& + e^{-\eta^{(i)}y}\Bigg\{\left[-\frac{1}{2}Ak(C_{5,s,2}+C_{6,d,1}) - \frac{B_{12}^2k}{2\omega\lambda'}G_2\right]\cos(\theta_1^{(0)}-\theta_2^{(0)}+\theta_r^{(1)}) \\
& - \left[\frac{1}{2}Ak(C_{6,s,1}+C_{5,d,2}) + \frac{B_{12}^2k}{2\omega\lambda'}G_2\right]\cos(\theta_2^{(0)}-\theta_1^{(0)}+\theta_r^{(1)}) + \left[\frac{1}{2}Ak(S_{5,s,2}-S_{6,d,1}) - \frac{B_{12}^2k}{2\omega\lambda'}G_5\right] \\
& \times\sin(\theta_1^{(0)}-\theta_2^{(0)}+\theta_r^{(1)}) + \left[\frac{1}{2}Ak(S_{6,s,1}-S_{5,d,2}) - \frac{B_{12}^2k}{2\omega\lambda'}G_5\right]\sin(\theta_2^{(0)}-\theta_1^{(0)}+\theta_r^{(1)}) \\
& - \frac{1}{2}Ak[(C_{5,s,1}+C_{6,s,2}+C_{5,d,1}+C_{6,d,2})\cos\theta_r^{(1)} - (S_{5,s,1}+S_{6,s,2}-S_{5,d,1}-S_{6,d,2})\sin\theta_r^{(1)}]\Bigg\} \\
& - \frac{1}{2}Ake^{-\mu^{(i)}y}\{(Q_{11}+Q_{21})\cos(\theta_1^{(0)}-\theta_r^{(2)}) + (Q_{12}+Q_{22})\cos(\theta_2^{(0)}-\theta_r^{(2)}) \\
& + (P_{11}+P_{21})\sin(\theta_1^{(0)}-\theta_r^{(2)}) + (P_{12}+P_{22})\sin(\theta_2^{(0)}-\theta_r^{(2)})\} \\
& + \frac{1}{2}Ak[C_{71}\cos(3\theta_1^{(0)}+\theta_2^{(0)}) + C_{82}\cos(3\theta_2^{(0)}+\theta_1^{(0)}) + (C_{72}+C_{81})\cos 2(\theta_1^{(0)}+\theta_2^{(0)})] \\
& + e^{-\eta^{(i)}y}\Bigg\{\left[\frac{1}{2}Ak(C_{5,s,2}+C_{6,s,1}) - \frac{B_{12}^2k}{2\omega\lambda'}G_3\right]\cos(\theta_1^{(0)}+\theta_2^{(0)}+\theta_r^{(1)}) \\
& - \left[\frac{1}{2}Ak(S_{5,s,2}+S_{6,s,1}) + \frac{B_{12}^2k}{2\omega\lambda'}G_4\right]\sin(\theta_1^{(0)}+\theta_2^{(0)}+\theta_r^{(1)}) + \frac{1}{2}Ak[C_{5,s,1}\cos(2\theta_1^{(0)}+\theta_r^{(1)})
\end{aligned}$$

$$+ C_{6,s,2}\cos(2\theta_2^{(0)} + \theta_r^{(1)}) - S_{5,s,1}\sin(2\theta_1^{(0)} + \theta_r^{(1)}) - S_{6,s,2}\sin(2\theta_2^{(0)} + \theta_r^{(1)})]\Big\}$$

$$+ \frac{1}{2}Ake^{-\mu^{(i)}y}\{(Q_{11} + Q_{21})\cos(\theta_1^{(0)} + \theta_r^{(2)}) + (Q_{12} + Q_{22})\cos(\theta_2^{(0)} + \theta_r^{(2)})$$

$$- (P_{11} + P_{21})\sin(\theta_1^{(0)} + \theta_r^{(2)}) - (P_{12} + P_{22})\sin(\theta_2^{(0)} + \theta_r^{(2)})\}. \quad (A.21)$$

The coefficients $C_{2+i,j}$ and $C_{6+i,j}$ have been written without the comma; for example, $C_{3,1} = C_{31}$. The first nine trigonometric functions plus the term $\sim G_5$ on the rhs of (A.21) are x and time independent.

REFERENCES

Anderson, D. L. T., and A. E. Gill, 1975: Spin-up of a stratified ocean with applications to upwelling. *Deep-Sea Res.*, **22**, 683–696.

Bender, C. M., and S. A. Orszag, 1978: *Advanced Mathematical Methods for Scientists and Engineers.* McGraw-Hill, 593 pp.

Chiswell, S., and R. Lukas, 1990: The Hawaii Ocean Time-Series (HOT). *Eos, Trans. Amer. Geophys. Union,* **71**(43), 1397.

——, E. Firing, D. Karl, R. Lukas, and C. Winn, 1990: Hawaii Ocean Time-Series program data report 1, 1988–1989. SOEST Tech. Rep. 1, School of Ocean and Earth Science and Technology, University of Hawaii, Honolulu, HI, 269 pp.

Gill, A. E., 1974: The stability of planetary waves on an infinite beta-plane. *Geophys. Fluid Dyn.*, **6**, 29–47.

Graef, F., 1993: First order resonance in the reflection of baroclinic Rossby waves. *J. Fluid Mech.*, **251**, 515–532.

——, 1994: Second order nonlinear interactions among Rossby waves. *Atmósfera*, **7**, 89–103.

Graef-Ziehl, F., 1990: Reflection of nonlinear baroclinic Rossby waves at a nonzonal boundary and the driving of secondary mean flows. Ph.D. dissertation, University of Hawaii, 283 pp.

Kang, Y. Q., and L. Magaard, 1980: Annual baroclinic Rossby waves in the central North Pacific. *J. Phys. Oceanogr.*, **10**, 1159–1167.

Karl, D., and C. Winn, 1991: A sea of change: Monitoring the oceans carbon cycle. *Environ. Sci. Technol.*, **25**, 1976–1981.

LeBlond, P. H., and L. A. Mysak, 1978: *Waves in the Ocean.* Elsevier, 602 pp.

Magaard, L., 1983: On the potential energy of baroclinic Rossby waves in the North Pacific. *J. Phys. Oceanogr.*, **13**, 38–42.

Mysak, L. A., and L. Magaard, 1983: Rossby wave driven Eulerian mean flows along non-zonal barriers, with application to the Hawaiian Ridge. *J. Phys. Oceanogr.*, **13**, 1716–1725.

Nayfeh, A. H., 1981: *Introduction to Perturbation Techniques.* Wiley-Interscience, 519 pp.

Oh, I. S., and L. Magaard, 1984: Rossby wave-induced secondary flows near barriers, with application to the Hawaiian Ridge. *J. Phys. Oceanogr.*, **14**, 1510–1513.

Pedlosky, J., 1979: *Geophysical Fluid Dynamics.* Springer-Verlag, 624 pp.

Plumb, R. A., 1977: The stability of small amplitude Rossby waves in a channel. *J. Fluid Mech.*, **80**, 705–720.

Roden, G. I., 1985: Mesoscale thermohaline structure in the vicinity of the Hawaiian Islands. *The Hawaiian Ocean Experiment. Proc. Hawaiian Winter Workshop,* Honolulu, Hawaii Institute of Geophysics, 139–160.

Sun, L. C., J. M. Price, L. Magaard, and G. Roden, 1988: The North Hawaiian Ridge Current: A comparison between an analytical theory and some prior observations. *J. Phys. Oceanogr.*, **18**, 384–388.

White, W. B., 1983: A narrow boundary current along the eastern side of the Hawaiian Ridge: The North Hawaiian Ridge Current. *J. Phys. Oceanogr.*, **13**, 1726–1731.

Winn, C., S. Chiswell, E. Firing, D. Karl, and R. Lukas, 1992: Hawaii Ocean Time-Series Program data report 2, 1990. SOEST Tech. Rep. 92-1, School of Ocean and Earth Science and Technology, University of Hawaii, Honolulu, HI, 175 pp.

——, R. Lukas, D. Karl, and E. Firing, 1993: Hawaii Ocean Time-Series Program data report 3, 1991. SOEST Tech. Rep. 93-3, School of Ocean and Earth Science and Technology, University of Hawaii, Honolulu, HI, 228 pp.